INFRARED HEAT TRANSFER BY ATMOSPHERIC WATER VAPOR

by ROBERT A. McCLATCHEY

B.Sc., Massachusetts Institute of Technology
(1960)

WITHDRAWN FROM MIT LIBRARIES

MASS. INST. TECH.
LIBRARY
LINDGREN

SUBMITTED IN PARTIAL FULFILLMENT OF THE REQUIREMENTS
FOR THE DEGREE OF MASTER OF SCIENCE
at the
MASSACHUSETTS INSTITUTE OF TECHNOLOGY
August 1961

Signature of Author ______________________________
Department of Meteorology, 21 August 1961

Certified by ______________________________
Thesis Supervisor

Accepted by ______________________________
Chairman, Departmental Committee on
Graduate Students

INFRARED HEAT TRANSFER BY ATMOSPHERIC WATER VAPOR

by
Robert A. McClatchey

Submitted to the Department of Meteorology
on 21 August 1961
in Partial Fulfillment of the Requirements
for the Degree of Master of Science

ABSTRACT

Empirical data on transmission functions are used to set up a general program to calculate the infrared radiation flux in the atmosphere in the two major regions of water vapor absorption. These empirical data are converted into analytic formulae and the problem is solved through the use of the IBM 709 computer. Results are obtained for several soundings and the corresponding cooling rates determined. These results are then compared with those obtained from the Elsasser Radiation Chart.

Thesis Supervisor: Henry G. Houghton
Title: Professor of Meteorology

Acknowledgements

The author gratefully acknowledges the invaluable advice and encouragement he received from Dr. L. D. Kaplan who also suggested the problem. Without Dr. Kaplan's extensive background information on infrared radiation this study could not have been undertaken. The author is also grateful to Professor Henry G. Houghton who served as thesis supervisor for his careful reading of the draft and for his suggestions.

TABLE OF CONTENTS

LIST OF TABLES AND FIGURES

LIST OF TABLES AND FIGURES (cont'd)

DEFINITION OF SYMBOLS

α = See Table 1.

B = Planck black body function

C_p = heat capacity at constant pressure

D = downward radiation flux

γ = line half-width

g = gravity

K = antilog α

k = absorption coefficient

$\mathcal{K} = \Sigma (S_i \gamma_i)^{1/2}$

m = mass of water vapor

ν = wave number

p = pressure

R = net upward radiation flux

S = line intensity

T = temperature

τ_f = diffuse transmission function

τ_r = beam transmission function

u = upward radiation flux

θ = zenith angle

w = m sec

x = $\Sigma S_i(T) / \Sigma S_i(T_0)$

y = $\left(\Sigma \left[S_i(T) \gamma_i(T) \right]^{1/2} / \Sigma \left[S_i(T_0) \gamma_i(T_0) \right]^{1/2} \right)^2$

I. INTRODUCTION

This paper is a semi-empirical general procedure for determining the net upward radiation flux in the infrared water vapor bands in the atmosphere. If this net upward flux is known at the various levels of a sounding, the flux divergence and time rate of change of temperature within a given level can be determined. Temperature and mass of absorber will be required at each pressure level. Between levels, the temperature and absorber parameters will be assumed to vary linearly with pressure.

The difficulty in the solution of the equation of radiative transfer is the dependence of the transmission function on pressure, temperature, wave number, and amount of absorbing material. Therefore, empirical data will be used to obtain a transmission function and to determine its variation with pressure, mass of water vapor, and spectral interval. A theoretical treatment will be introduced to account for the temperature dependence of the transmission.

II. GENERAL RADIATION THEORY

The solution to the radiative transfer problem for an atmosphere of arbitrary constitution is stated by Elsasser (1942) as follows, giving the flux arriving at $m = m_o$ from the region between m_o and m_1:

$$F = -\int_0^\infty d\nu \int_{m_o}^{m_1} \pi B \frac{d}{dm} \tau_f (m - m_o)\, dm \tag{1}$$

where m = mass of water vapor, τ = transmission,

ν = wave number, B = Planck black body function.

Integrating equation (1) by parts and adding a constant of integration, we have for the flux arriving at a level m_o from the layer between m_o and m_1:

$$F = -\int_0^\infty \pi B(m_1)\, \tau(m_1 - m_o)\, d\nu + \int_0^\infty \pi B(m_o)\, d\nu$$
$$+ \int_{m_o}^{m_1} dm \int_0^\infty \frac{d(\pi B)}{dm} \tau\, d\nu + C \tag{2}$$

Converting the independent variable from m to T, where T = temperature, we have:

$$\int dm \int_0^\infty \frac{d(\pi B)}{dm} \tau\, d\nu = \int dT \int_0^\infty \frac{d(\pi B)}{dT} \tau\, d\nu$$

So,

$$F = -\int_0^{\infty} \pi B(T_1)\,\tau(T_1 - T_0)\,d\nu + \int_0^{\infty} \pi B(T_0) + \int_{T_0}^{T_1} dT \int \frac{d(\pi B)}{dT}\,\tau(T_0 - T)\,d\nu + C \tag{3}$$

Consider the following picture:

T_∞

T_Z

T_G = SURFACE TEMP.

It is desired to determine the net upward flux across the level Z. The upward flux will be given by an expression like (3) above but with T_o replaced by T_z and T_1 replaced by T_g, the temperature of the surface.

$$U = -\int_0^{\infty} \pi B(T_G)\,\tau(T_G - T_Z)\,d\nu + \int \pi B(T_Z)\,d\nu + \int_{T_Z}^{T_G} dT \int_0^{\infty} \frac{d(\pi B)}{dT}\,\tau(T_Z - T)\,d\nu + C \tag{4}$$

The integration constant must yet be determined. This can be done from the condition that $U = \int_0^{\infty} \pi B(T_G)\,\tau(T_G - T_Z)\,d\nu$ near the surface where $\Delta m \rightarrow 0$, $T = T_z$ can be replaced by T_g and $\tau \rightarrow 1$.

Therefore, the above expression, valid an infinitesimal distance from the surface, becomes (noting that the interval of integration is also infinitesimal):

$$\int_0^\infty \pi B(T_G)\,\tau(T_G-T_Z)\,d\nu = -\int_0^\infty \pi B(T_G)\,\tau(T_G-T_Z)\,d\nu$$
$$+\int_0^\infty \pi B(T_Z)\,d\nu + \int_0^\infty \pi B(T_G)\,\tau(T_Z-T_G)\,d\nu$$
$$-\int_0^\infty \pi B(T_Z)\,\tau(T_Z-T_Z)\,d\nu + \text{CONSTANT}$$

It should be clear that $\tau(T_G-T_Z)\equiv\tau(T_Z-T_G)$ and also that $\tau(T_Z-T_Z)\equiv 1$.

Therefore, we have: Constant = $\int_0^\infty \pi B(T_G)\,\tau(T_G-T_Z)\,d\nu$

And,

$$U=\int_0^\infty \pi B(T_Z)\,d\nu+\int_{T_Z}^{T_G} dT\int_0^\infty \frac{d(\pi B)}{dT}\,\tau(T_Z-T)\,d\nu \tag{5}$$

The downward radiation flux can be expressed similarly using equation (3) as starting point, but T_g must be replaced by T_∞ .

$$D=-\int_0^\infty \pi B(T_\infty)\,\tau(T_\infty-T_Z)\,d\nu+\int_0^\infty \pi B(T_Z)\,d\nu$$
$$+\int_{T_Z}^{T_\infty} dT\int_0^\infty \frac{d(\pi B(T))}{dT}\,\tau(T_Z-T)\,d\nu + \text{CONSTANT} \tag{6}$$

In order to determine the constant of integration here, two situations must be considered, the one in which T_∞ refers to a region where no more absorber exists, and the one in which T_∞ refers to a cloud base. The first situation is quite easy: $T_z \rightarrow T_\infty$, $\tau(T_\infty-T_Z)\rightarrow\tau(T_\infty-T_\infty)=1$, and D must be zero. Therefore, all terms in equation (6) must add to zero, and the constant of integration is itself equal to zero. If T_∞ refers to a cloud base, however, the expression becomes exactly analogous to the one for the upward flux except with T_g replaced by T_∞. In this case the constant of integration is $\int_0^\infty \pi B(T_\infty)\,\tau(T_\infty - T_z)\,d\nu$.

The following expressions for the downward flux at level "Z" are thus obtained:

Without cloud cover:

$$D = -\int_0^\infty \pi B(T_\infty)\,\tau(T_\infty - T_z)\,d\nu + \int_0^\infty \pi B(T_z)\,d\nu + \int_{T_z}^{T_\infty} dT \int_0^\infty \frac{d(\pi B(T))}{dT}\,\tau(T_z - T)\,d\nu \tag{7}$$

With cloud cover:

$$D = \int_0^\infty \pi B(T_z)\,d\nu + \int_{T_z}^{T_\infty} dT \int_0^\infty \frac{d(\pi B)}{dT}\,\tau(T_z - T)\,d\nu \tag{8}$$

Summing the upward and downward radiation fluxes will result in the following net upward radiation flux (R_z) at level z:

Without overcast (equation (5) minus (7)):

$$R_z = \int_{T_\infty}^{T_G} dT \int_0^\infty \frac{d(\pi B(T))}{dT}\,\tau(T_z - T)\,d\nu + \int_0^\infty \pi B(T_\infty)\,\tau(T_\infty - T_z)\,d\nu \tag{9}$$

With overcast (equation (5) minus (8)):

$$R_z = \int_{T_\infty}^{T_G} dT \int_0^\infty \frac{d\,\pi B(T)}{dT}\,\tau(T_z - T)\,d\nu \tag{10}$$

Equations (9) and (10) are the basic equations, the solution of which comprises the remainder of this report.

In finite difference form, for computational purposes, equations (9) and (10) become:

$$R_z = \sum_{\nu} \left\{ \sum_{B(T_\infty)}^{B(T_G)} \tau(T_z - T)\,\Delta(\pi B) \right\} \Delta\nu + \sum_{\nu} \pi B(T_\infty)\,\tau(T_\infty - T_z)\,\Delta\nu \qquad (9')$$

$$R_z = \sum_{\nu} \left\{ \sum_{B(T_\infty)}^{B(T_G)} \tau(T_z - T)\,\Delta(\pi B) \right\} \Delta\nu \qquad (10')$$

Once the net upward flux (R) is determined, the radiative cooling can be evaluated from the relation $\frac{\partial T}{\partial t} = -\frac{g}{C_p}\frac{\partial R}{\partial P}$.

Others have devised various theoretical and experimental methods of solving these equations. The black body flux, B, is a well-known function, but the difficult term to evaluate is the transmission, τ .

III. DETERMINATION OF THE TRANSMISSION FUNCTION

The transmission is a complicated function of wave number, pressure, temperature and amount of absorber. Thus, a theoretical justification will be given for determining τ, although the final analysis will make direct use of experimentally determined values of transmission.

The following summary of a paper by Godson and comments by Curtis (both unpublished) should serve to indicate the method of considering the pressure, temperature, and absorber dependence of the transmission for a given wave number interval.

For transmission through thin layers:

In general, the transmission through a layer of thickness m for a frequency interval of infinitesimal width is given by the exponential expression

$$\tau_\nu = \exp - \int k_\nu \, dm$$

where k_ν is the absorption coefficient at wave number ν and the integral recognizes the variability of k_ν with m or with parameters such as pressure and temperature which may be expressed as functions of m. For a thin layer for which τ_ν is not too different from unity we may write

$$\tau_\nu = 1 - \int k_\nu \, dm$$

The average transmission for a thin layer over a band of width $\Delta\nu$ that contains i spectral lines is given by

$$\tau_I = 1 - \frac{\iint \Sigma k_i \, d\nu \, dm}{\Delta \nu}$$

The intensity of a line S_i is defined by

$$S_i = \int_{-\infty}^{\infty} k_i \, d\nu$$

Substituting

$$\tau_I = 1 - \frac{\int \Sigma S_i \, dm}{\Delta \nu}$$

An effective mass of absorber is defined as follows:

$$m_e \sum_i S_i(T_0) = \int \sum_i S_i(T) \, dm$$

$$m_e = \frac{\int \sum_i S_i(T) \, dm}{\sum_i S_i(T_0)} = \int \chi \, dm \quad \text{where } x = \frac{\Sigma S_i(T)}{\Sigma S_i(T_0)} \tag{11}$$

The quantity "x" will depend on the spectral interval as well as on the temperature. This function "x" has been determined theoretically and curves of x vs T are included for specified spectral intervals.

Kaplan (1953), using a model assuming random line-position, obtained the following transmission for a homogeneous path:

$$\tau_I = \exp\left\{-\frac{1}{\Delta\nu}\sum_i \int_{-\infty}^{+\infty}\left[1-e^{-k_{\nu_i} m}\right] d(\nu-\nu_i)\right\}$$

For Lorentz lines, this equation becomes:

$$\tau_I = \exp\left\{-\frac{2\pi}{\Delta\nu}\sum \gamma_i x_i e^{-x_i}\left[I_0(x_i)+I_1(x_i)\right]\right\}$$

where I_0 and I_1 are Bessel functions of imaginary argument and

$x_i = \frac{S_i m}{2\pi\gamma_i}$ where γ_i = half-width of the i^{th} line.

When examined for large argument, we have:

$$I_0(x_i)+I_1(x_i) \approx \frac{2e^{x_i}}{(2\pi x_i)^{1/2}}$$

So,

$$\tau_I = \exp-\left[\frac{2\pi}{\Delta\nu}\sum_i \frac{2x_i^{1/2}\gamma_i}{(2\pi)^{1/2}}\right]$$

$$= \exp-\left[\frac{2}{\Delta\nu}\sum_i (S_i m \gamma_i)^{1/2}\right]$$

In order to consider an arbitrary distribution of m and noting that γ_i is proportional to pressure, integration with respect to m and the setting of $\gamma_i = \gamma_{o_i}\frac{p_i}{p_o}$ is justified. Thus, we have:

$$\tau_I = \exp-\left[\frac{2}{\Delta\nu}\sum_i\left(\int_{m_o}^{m} S_i(T)\gamma_{o_i}(T)\frac{p}{p_o}\,dm\right)^{1/2}\right]$$

But, this above is the same as for m_e all at T_o and p_e if

$$\sum_i \left(\int S_i(T)\,\gamma_i(T)\,\frac{p}{p_o}\,dm \right)^{1/2}$$

$$= \left(\frac{p_e m_e}{p_o} \right)^{1/2} \sum_i \left(S_i(T_o)\,\gamma_i(T_o) \right)^{1/2}$$

Thus, for this model,

$$p_e m_e = \left\{ \frac{\sum_i \left(\int S_i(T)\,\gamma_i(T)\,p\,dm \right)^{1/2}}{\sum_i \left(S_i(T_o)\,\gamma_i(T_o) \right)^{1/2}} \right\}^2 \tag{12}$$

This expression is inconvenient as it stands, since the integral has to be evaluated separately for each line, the $S\gamma$ product having a different temperature dependence for each line.

In order to obtain a more usable expression, consider a homogeneous layer at p_j, T_j, containing mass dm_j.

Using (12), the contribution to $p_e m_e$ is:

$$d(p_e m_e)_j = \left\{ \frac{\sum_i \left([S_i(T)\,\gamma_i(T)]\,p_j\,dm_j \right)^{1/2}}{\sum_i \left([S_i(T_o)\,\gamma_i(T_o)] \right)^{1/2}} \right\}^2$$

$$= \left\{ \frac{\sum_i \left(S_i(T)\,\gamma_i(T) \right)_j^{1/2}}{\sum_i \left(S_i(T_o)\,\gamma_i(T_o) \right)^{1/2}} \right\}^2 p_j\,dm_j = y_j\,p_j\,dm_j \tag{13}$$

where $$y_j = \left\{ \frac{\sum_i \left[S_i(T)\gamma_i(T) \right]^{1/2}}{\sum_i \left[S_i(T_0)\gamma_i(T_0) \right]^{1/2}} \right\}^2 \qquad (14)$$

Thus, we have a much more convenient form in which the values of y_j can be determined theoretically from the above and then y can be graphed as a function of T for a given wave-number interval.

$$p_e m_e = \int y p \, dm \qquad (15)$$

This above treatment allows an effective mass to be determined for thin layers and an effective pm product to be determined for thick layers, thus yielding correct transmissions for both of these cases.

Equation (15) will be used along with equation (11) to determine an effective pressure at which to place all the absorber. This will constitute a temperature correction which can be applied as soon as the pressure, temperature and amount of absorbing material are known. In this way, both the $p_e m_e$ product and the effective pressure itself can be determined for each sounding.

The procedure will be to determine $p_e m_e$ and p_e from the sounding through a given slice of atmosphere; then to go to experimental curves of transmission to determine the values of τ required for the numerical integration in equations (9') and (10').

IV. THE ROTATIONAL BAND

The rotational band is located in the wave-number region 0-600. Later in the report, the rotation-vibration band will be considered. It is centered at 1595 cm^{-1} and contains two symmetric sides, the shapes of each being similar to the rotational band.

Palmer (1960) has experimentally measured transmission of water vapor for various values of pressure and mass of absorber in the rotational band.

He has also done some work at different temperatures, although his temperature spread is not sufficient to draw any conclusions for comparison with the preceding theoretical discussion.

On the following pages Palmer's curves of transmission vs log mp are displayed for some of the spectral intervals to be used in the numerical integration. Notice that the high pressure ($\sim$60 cm of Hg) curves are slightly above the low pressure curves in all cases. Comparing the curves in these spectral intervals indicates that a generalized curve might be used for each of these two pressures. These curves could then be displaced appropriately to right or left along the log mp axis depending on the spectral interval. This idea of a generalized curve was first proposed by Cowling (1950).

Expressions have been determined for both the high and low pressure curves in order that this whole problem might be programmed and run on the IBM 709 computer. Then initial data of a sounding might be punched on cards and the resulting radiation fluxes immediately determined. The

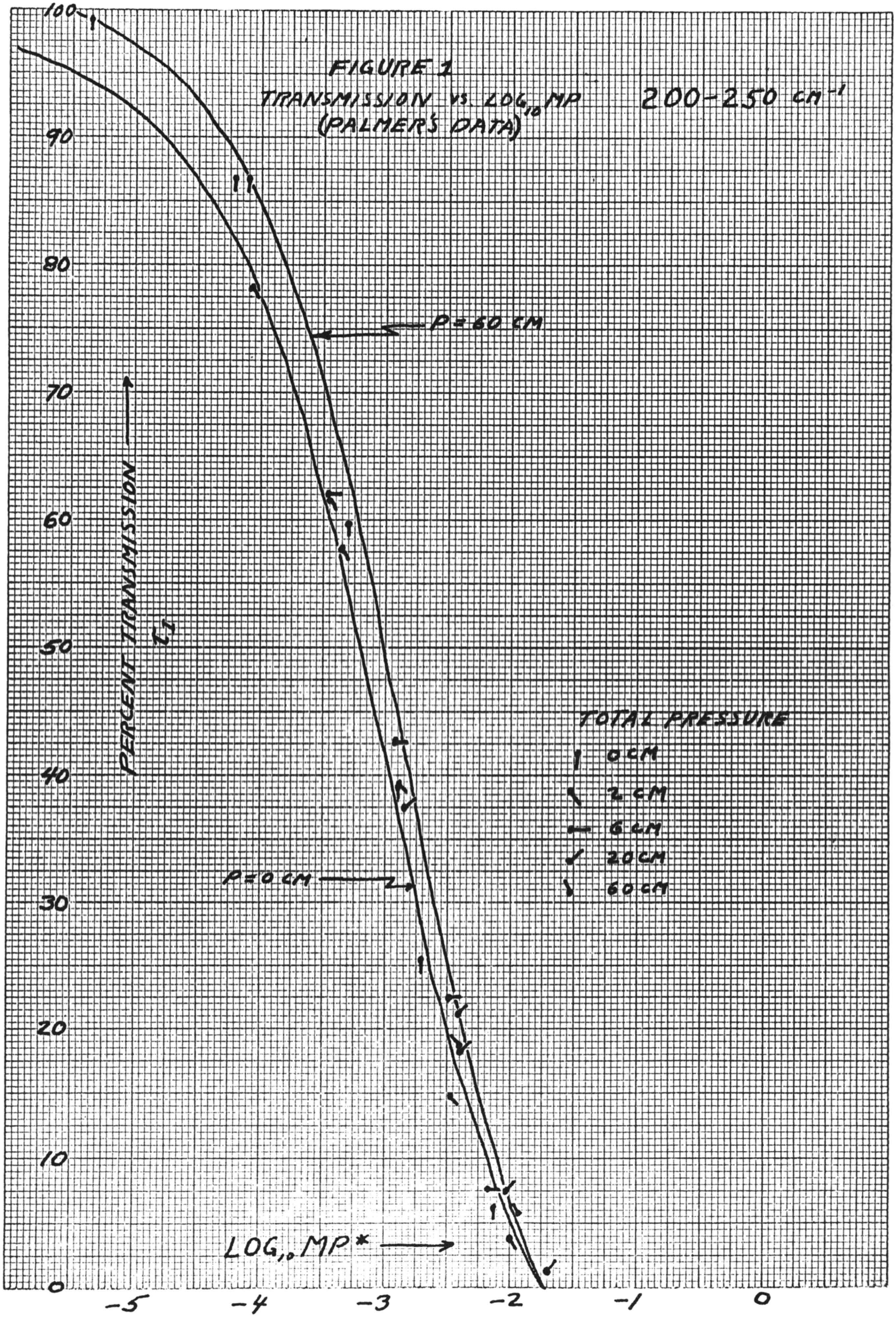
FIGURE 1
TRANSMISSION VS. $LOG_{10} MP$
(PALMER'S DATA)
200-250 CM^{-1}
P = 60 CM
P = 0 CM
PERCENT TRANSMISSION
τ_I
TOTAL PRESSURE
0 CM
2 CM
6 CM
20 CM
60 CM
$LOG_{10} MP^*$
100
90
80
70
60
50
40
30
20
10
0
-5
-4
-3
-2
-1
0

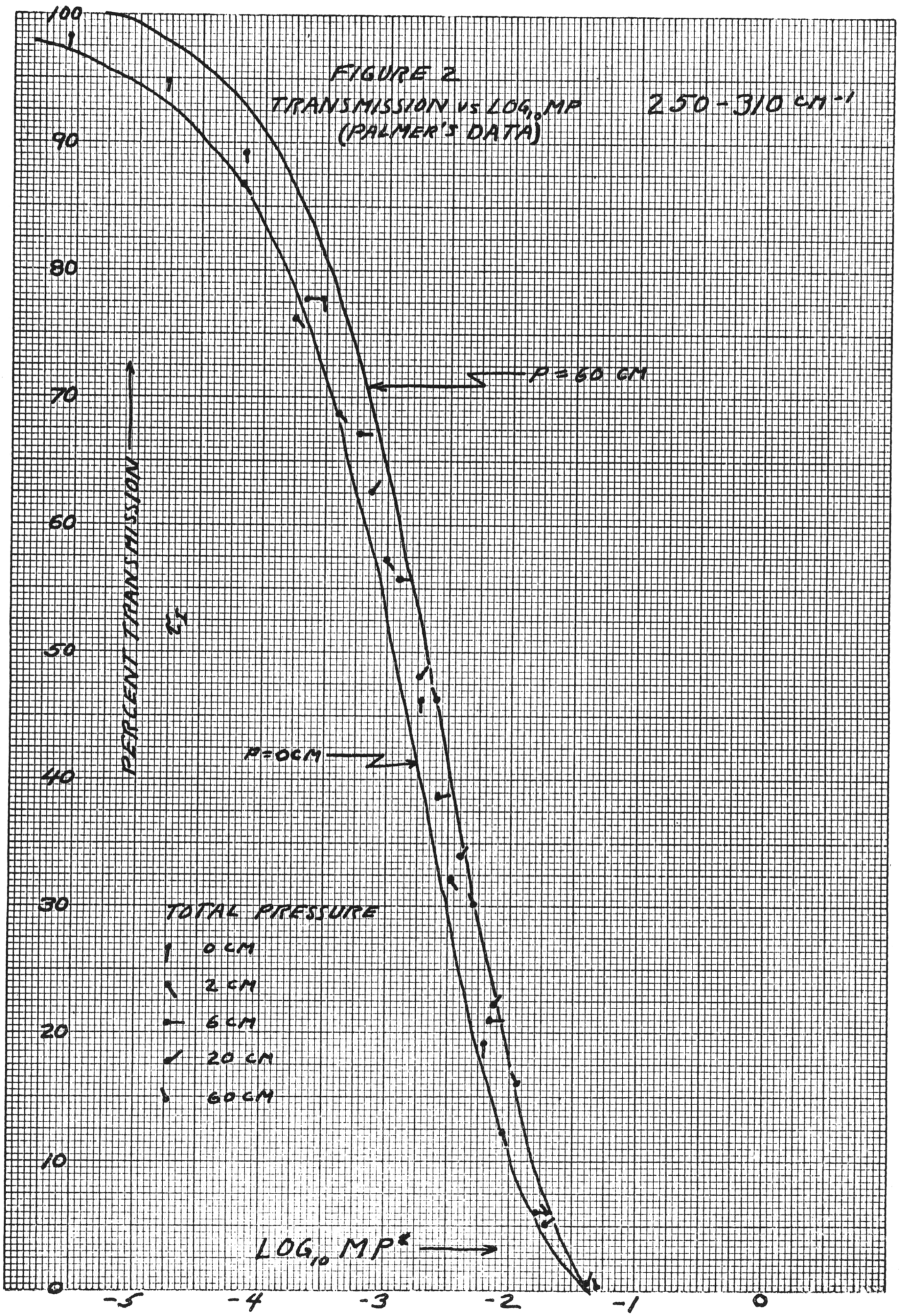
FIGURE 2
TRANSMISSION vs LOG₁₀ MP
(PALMER'S DATA)
250-310 CM⁻¹
P=60 CM
P=0CM
PERCENT TRANSMISSION
TOTAL PRESSURE
0 CM
2 CM
6 CM
20 CM
60 CM
LOG₁₀ MP*
100
90
80
70
60
50
40
30
20
10
0
-5
-4
-3
-2
-1
0

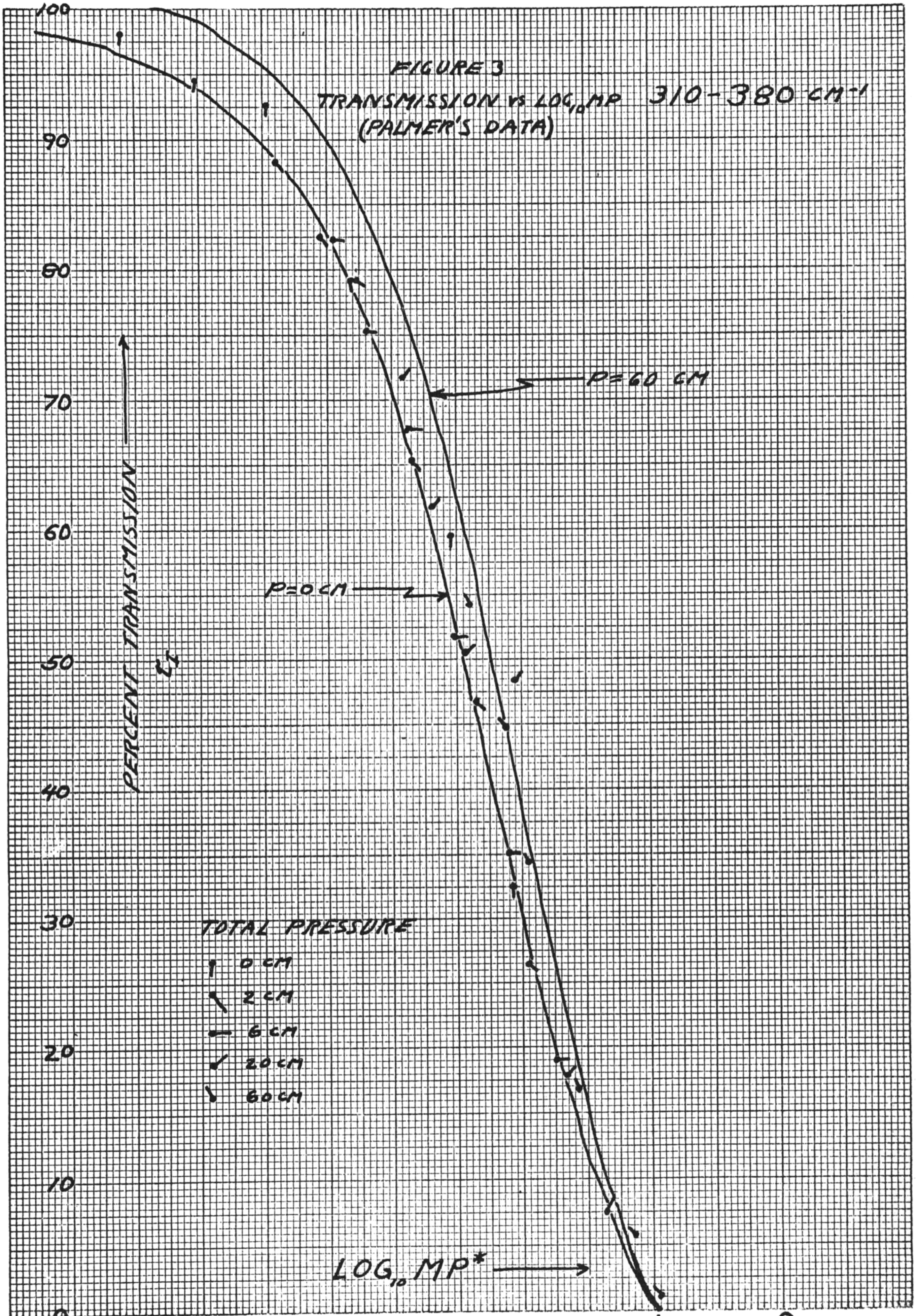
FIGURE 3
TRANSMISSION vs LOG_{10} MP
(PALMER'S DATA)
310-380 CM-1
P=60 CM
P=0 CM
PERCENT TRANSMISSION
TOTAL PRESSURE
0 CM
2 CM
6 CM
20 CM
60 CM
LOG_{10} MP*
100
90
80
70
60
50
40
30
20
10
0
-5
-4
-3
-2
-1
0

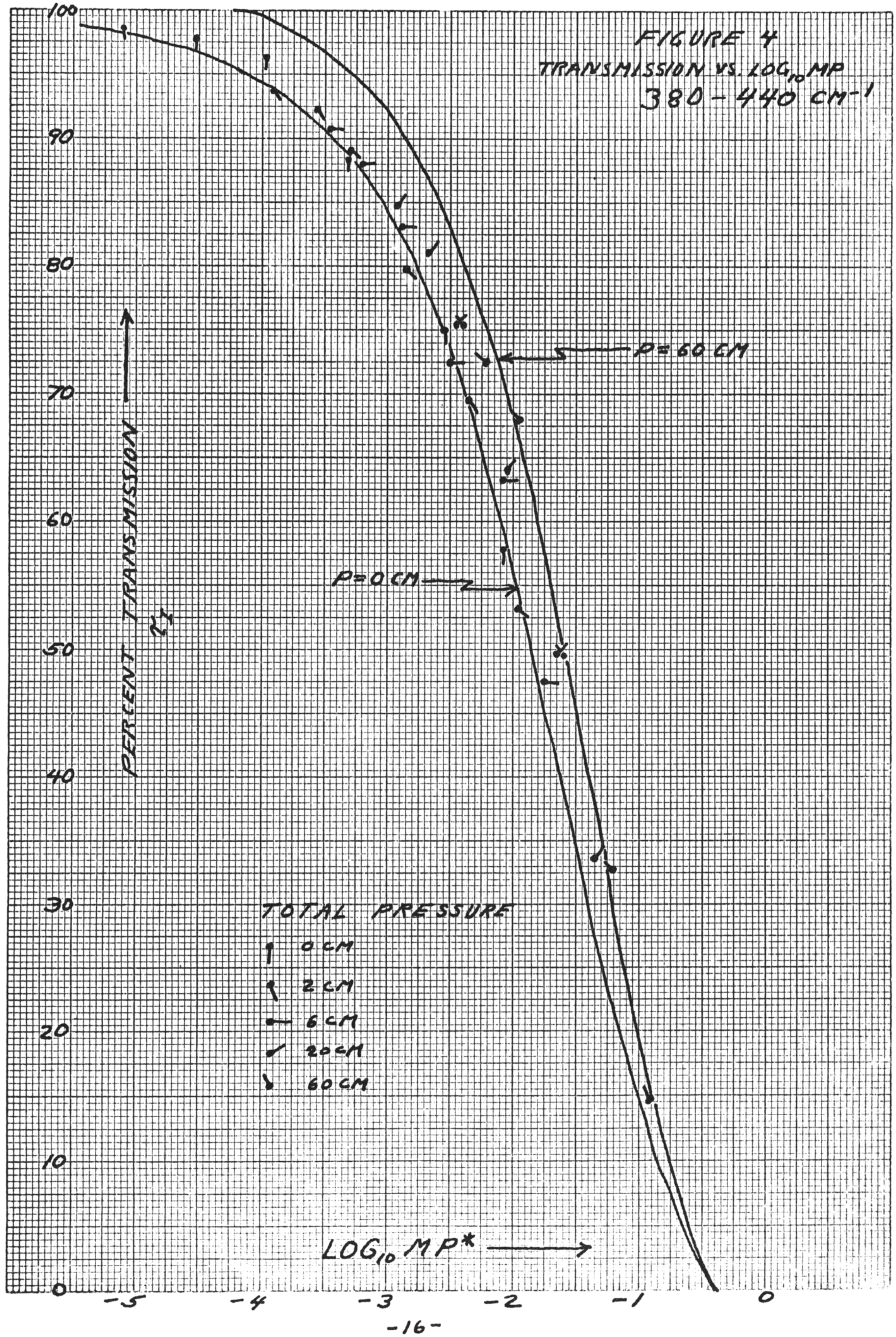
FIGURE 4
TRANSMISSION VS. LOG_{10} MP
380 - 440 CM^{-1}
P = 60 CM
P = 0 CM
PERCENT TRANSMISSION
TOTAL PRESSURE
0 CM
2 CM
6 CM
20 CM
60 CM
LOG_{10} MP*
100
90
80
70
60
50
40
30
20
10
0
-5
-4
-3
-2
-1
0

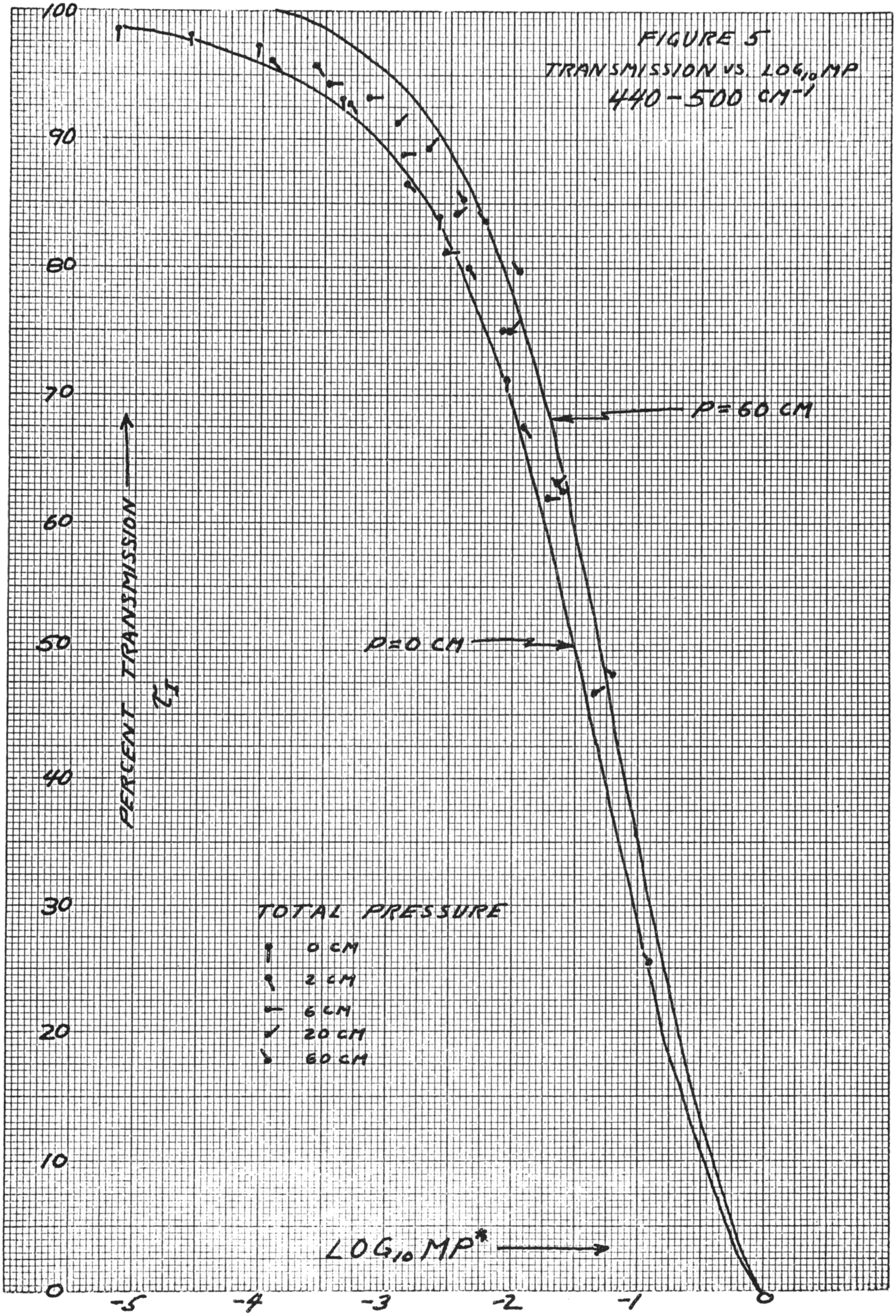
FIGURE 5
TRANSMISSION VS. LOG10 MP
440-500 CM-1
P=60 CM
P=0 CM
PERCENT TRANSMISSION
TOTAL PRESSURE
0 CM
2 CM
6 CM
20 CM
60 CM
LOG10 MP*
100
90
80
70
60
50
40
30
20
10
0
-5
-4
-3
-2
-1
0

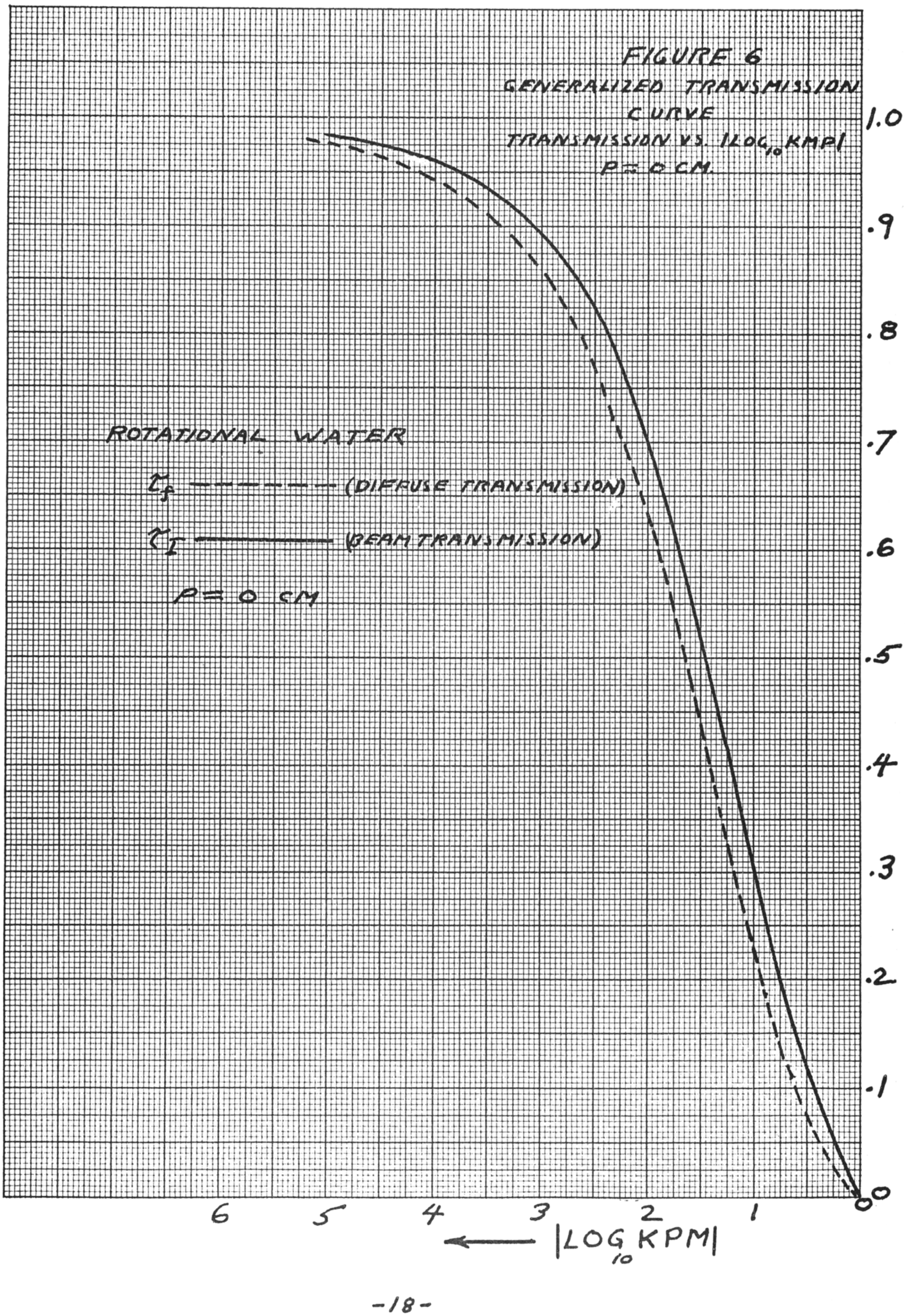

FIGURE 6
GENERALIZED TRANSMISSION CURVE
TRANSMISSION VS. |LOG10 KMP|
P = 0 CM.
ROTATIONAL WATER
τf (DIFFUSE TRANSMISSION)
τI (BEAM TRANSMISSION)
P = 0 CM
1.0
.9
.8
.7
.6
.5
.4
.3
.2
.1
0
τ
6
5
4
3
2
1
0
|LOG10 KPM|

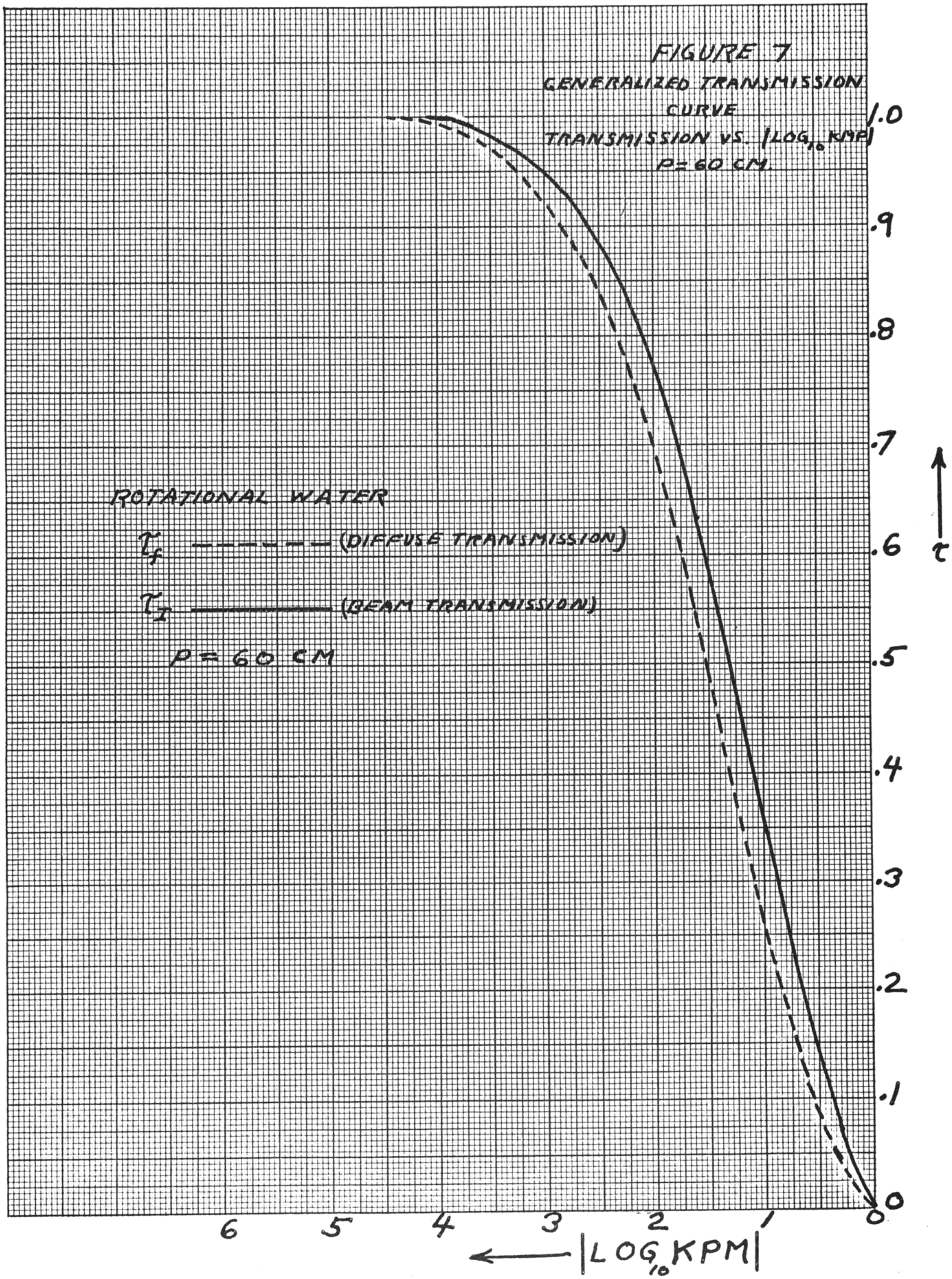
FIGURE 7
GENERALIZED TRANSMISSION CURVE
TRANSMISSION VS. |LOG10 KMP|
P = 60 CM.
ROTATIONAL WATER
τ_f ------- (DIFFUSE TRANSMISSION)
τ_I ——— (BEAM TRANSMISSION)
P = 60 CM
1.0
.9
.8
.7
.6
.5
.4
.3
.2
.1
0
τ
6
5
4
3
2
1
0
|LOG10 KPM|

empirical expressions used (which give a very good fit) are as follows:

High pressure curve (p = .79 atm. = 802 mb):

$$\tau_I = \frac{x^3 + .7x^2 + 1.5x}{x^3 + .6x^2 + 7.4} \tag{16}$$

Low pressure curve (p = 0 atmospheres):

$$\tau_I = \frac{x^3 + .1x^2 + 1.5x}{x^3 + .2x^2 + 7.4} \tag{17}$$

where the subscript I refers to beam transmission, and where $x = |Z - \alpha|$ and $Z = \log_{10} mp$, and α is tabulated below for the various spectral intervals.

Table 1. Values of α which displace the generalized curve of Figures 6 and 7 to left or to right appropriately.

SPECTRAL INTERVAL (cm^{-1})	ALPHA
620 - 680	+1.45
560 - 620	+ .86
500 - 560	+ .37
440 - 500	- .02
380 - 440	- .40
310 - 380	- .99
250 - 310	-1.40
200 - 250	-1.73
150 - 200	-1.80
100 - 150	-1.92
50 - 100	-1.85

The transmissions in the region from 500-200 cm^{-1} have been experimentally determined in 5 cm^{-1} intervals by Palmer. The displacements of the generalized curves (Equations (16) and (17)) for the regions greater than 500 cm^{-1} and less than 200 cm^{-1} have been determined from the following theoretical argument:

For a narrow spectral region $\tau = exp(-k\sqrt{mp})$ where $k = \sum_i (S_i \gamma_i)^{1/2}$. The constant k can be determined theoretically from quantum mechanics. Taking logarithms of the above expression for the transmission, we have:

$$\log_e \tau = -k\sqrt{mp} \quad : \quad (\log_e \tau)^2 = k^2 mp$$

For a different spectral interval, we will in general have $(\log_e \tau')^2 = k'^2 (mp)'$. However, if the curve is to move to right or left as a whole, the change in log mp must be determined at constant τ. So, placing $\tau = \tau'$ above, we have:

$$k^2 mp = k'^2 (mp)' \quad \text{or} \quad (mp)' = \left(\frac{k}{k'}\right)^2 mp$$

Taking $\log_{10}$ of the result gives:

$$\log_{10} (mp)' = 2 \log_{10} \left(\frac{k}{k'}\right) + \log_{10} mp$$

So, the displacement of the generalized curve from the 500-560 region to the 560-620 region is found by simply adding 2 log ($\frac{k}{k'}$) to each point on the curve at constant transmission.

The values of k for the various spectral intervals are listed below:

Table 2. The quantity (k) necessary to determine the theoretical position of the transmission function for a given spectral interval.

SPECTRAL INTERVAL (cm^{-1})	$K = \sum_i (S_i \gamma_i)^{1/2}$
620 - 680	15.39
560 - 620	28.14
500 - 560	48.47
440 - 500	85.21
380 - 440	144.43
310 - 380	359.96
250 - 310	518.04
200 - 250	727.82
150 - 200	755.42
100 - 150	924.07
50 - 100	838.77

In order to set up this problem for programming, the curves of x and y vs T for all spectral regions of interest must also be written down as analytic functions. This has been done and the results appear in Table 3.

For computation purposes, the fact that Palmer's data are determined at many temperatures leads to the necessity of a further correction to the above treatment. The transmission in the spectral region from 500 - 380 cm^{-1} will be taken as valid at 19°C. (This is about the average temperature of the experimental data.) The spectral region from 380 - 250 cm^{-1} can be taken as experimentally valid at 10°C. Similarly, the region from 250 - 200 cm^{-1} will be valid at 19°C. The spectral regions either greater than 500 cm^{-1} or less than 200 cm^{-1} will be taken as valid at T = 19°C because the extrapolation is taken from both ends of the experimentally determined region.

TABLE 3

ROTATIONAL BAND TEMPERATURE CORRECTION FACTORS

$\Delta\nu$ cm^{-1}	"y" CORRECTION	"X" CORRECTION
50-100	$y = 1.60 \times 10^{3}(T+273)^{-1.31}$	$x = 1.55 \times 10^{3}(T+273)^{-1.30}$
100-150	$y = 7.78(T+273)^{-.364}$	$x = 1.608 - .00217(T+273)$
150-200	$y = .0757(T+273)^{.458}$	$x = 1.0$
200-250	$y = 1.02 \cos\left(\frac{T-40}{767}\right)$	$x = \cos\left[\frac{T-17}{220}\right]$
250-310	$y = 1.28 \cos\left[\frac{T-145}{1.91}\right]$	$x = 1.25 \cos\left[\frac{T-115}{168}\right]$
310-380	$y = .8 + .62 \cos\left[\frac{T-119}{81.9}\right]$	$x = 1.20 - 1.10 \cos\left[\frac{T+148}{111.3}\right]$
380-440	$y = 1.1 - \cos\left[\frac{T+121}{93.9}\right]$	$x = 5.75 \times 10^{-10}(T+273)^{3.77}$
440-500	$y = 1.1 - .95 \cos\left[\frac{T+102}{80.9}\right]$	$x = .17 + 4.05 \times 10^{-5}(T+136)^{2}$
500-560	$y = 1.0 - .9 \cos\left[\frac{T+97}{72.6}\right]$	$x = .1 + 4.72 \times 10^{-5}(T+132)^{2}$
560-620	$y = 2.285 \times 10^{-10}(T+273)^{3.94}$	$x = 2.00 \times 10^{-10}(T+273)^{3.96}$
620-680	$y = 5.010 \times 10^{-12}(T+273)^{4.618}$	$x = 3.48 \times 10^{-12}(T+273)^{4.68}$

The curves corresponding to these expressions are found on the following pages in figures 8 -11.

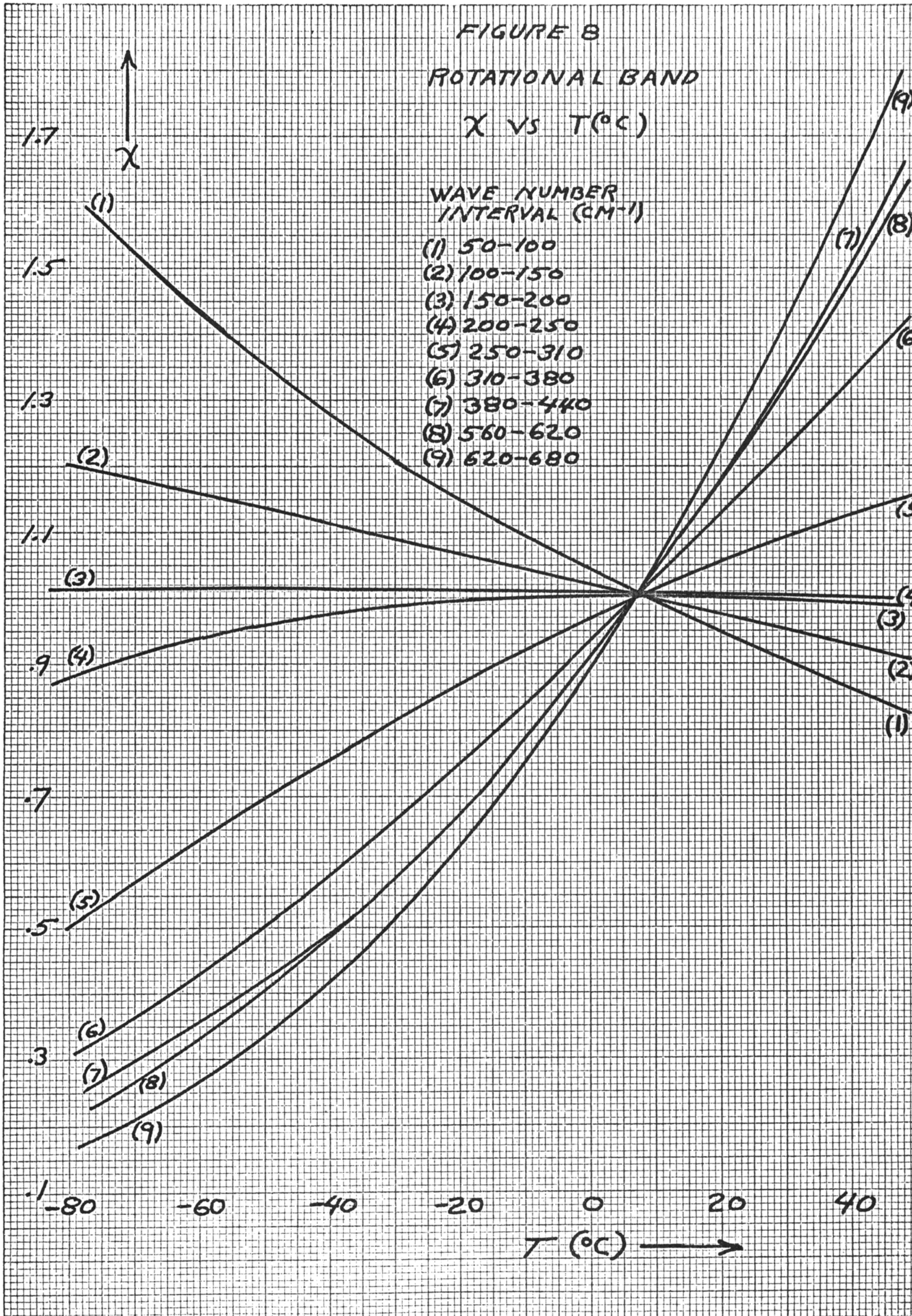
FIGURE 8
ROTATIONAL BAND
χ VS T(°C)
WAVE NUMBER
INTERVAL (CM-1)
(1) 50-100
(2) 100-150
(3) 150-200
(4) 200-250
(5) 250-310
(6) 310-380
(7) 380-440
(8) 560-620
(9) 620-680
χ
1.7
1.5
1.3
1.1
.9
.7
.5
.3
.1
-80
-60
-40
-20
0
20
40
T (°C)
(1)
(2)
(3)
(4)
(5)
(6)
(7)
(8)
(9)

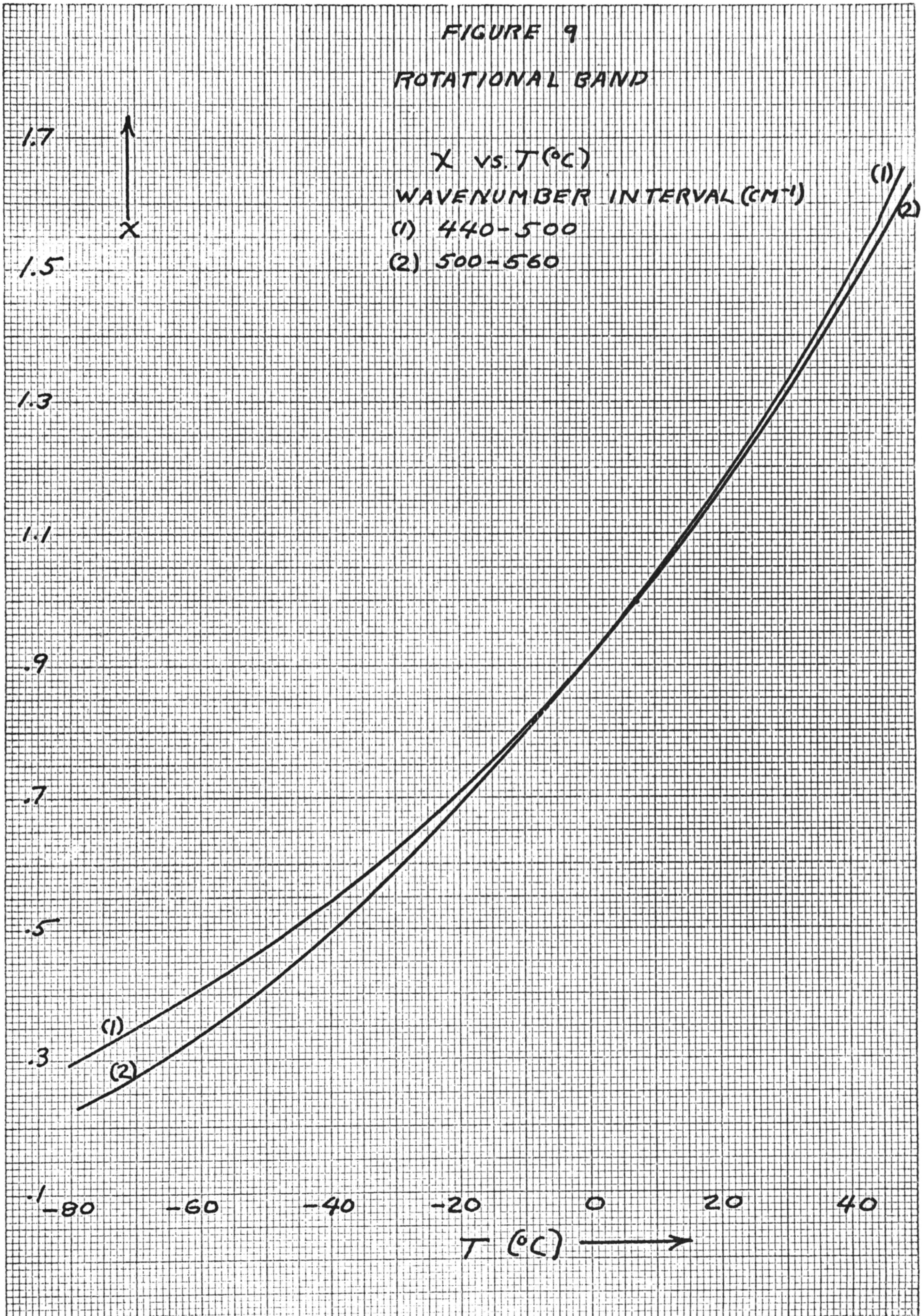
FIGURE 9
ROTATIONAL BAND
χ vs. T (°C)
WAVENUMBER INTERVAL (CM⁻¹)
(1) 440-500
(2) 500-560
χ
1.7
1.5
1.3
1.1
.9
.7
.5
.3
.1
-80
-60
-40
-20
0
20
40
T (°C)
(1)
(2)

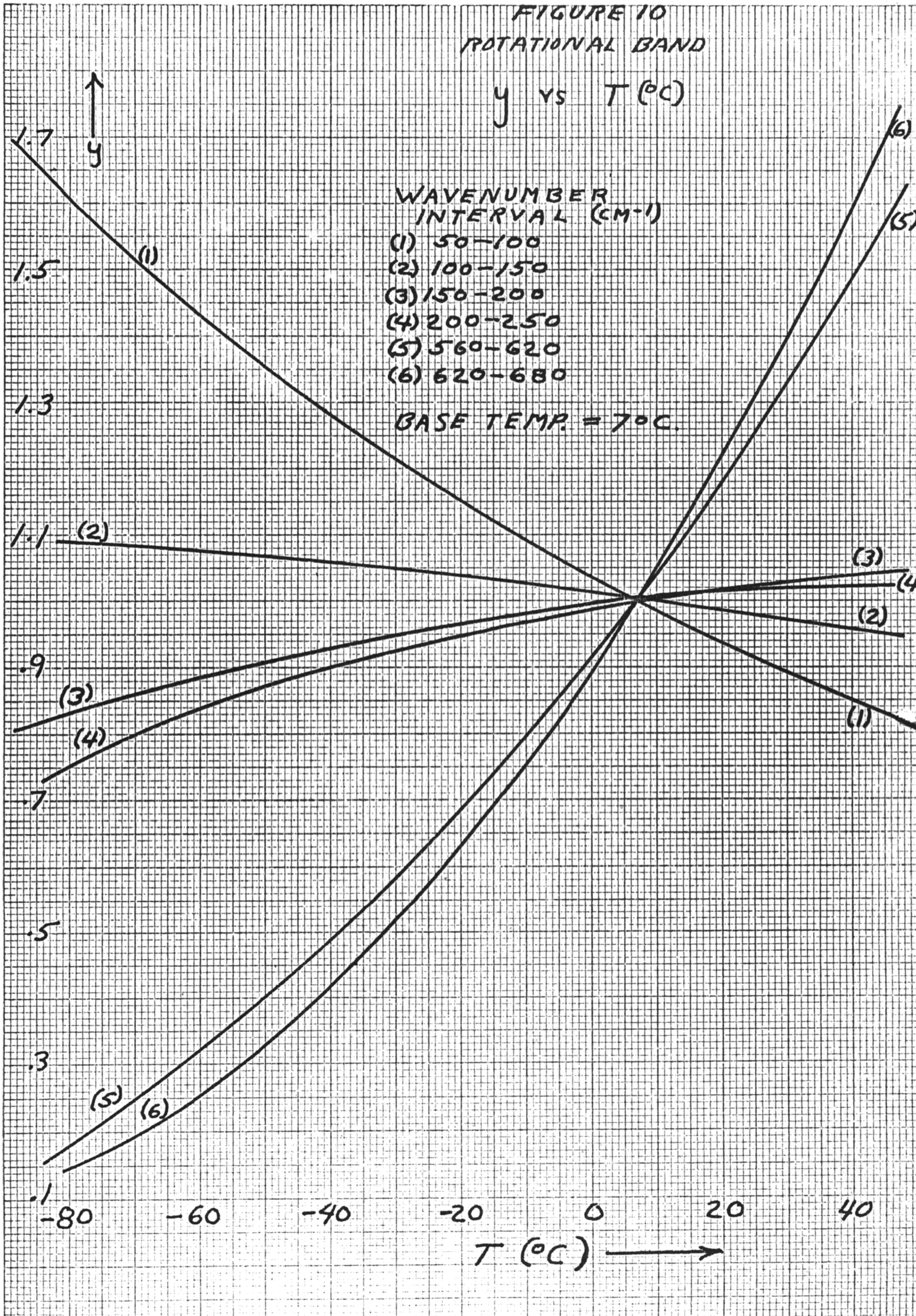
FIGURE 10
ROTATIONAL BAND
y vs T (°C)
WAVENUMBER INTERVAL (CM-1)
(1) 50-100
(2) 100-150
(3) 150-200
(4) 200-250
(5) 560-620
(6) 620-680
BASE TEMP. = 7°C.
y
1.7
1.5
1.3
1.1
.9
.7
.5
.3
.1
-80
-60
-40
-20
0
20
40
T (°C)

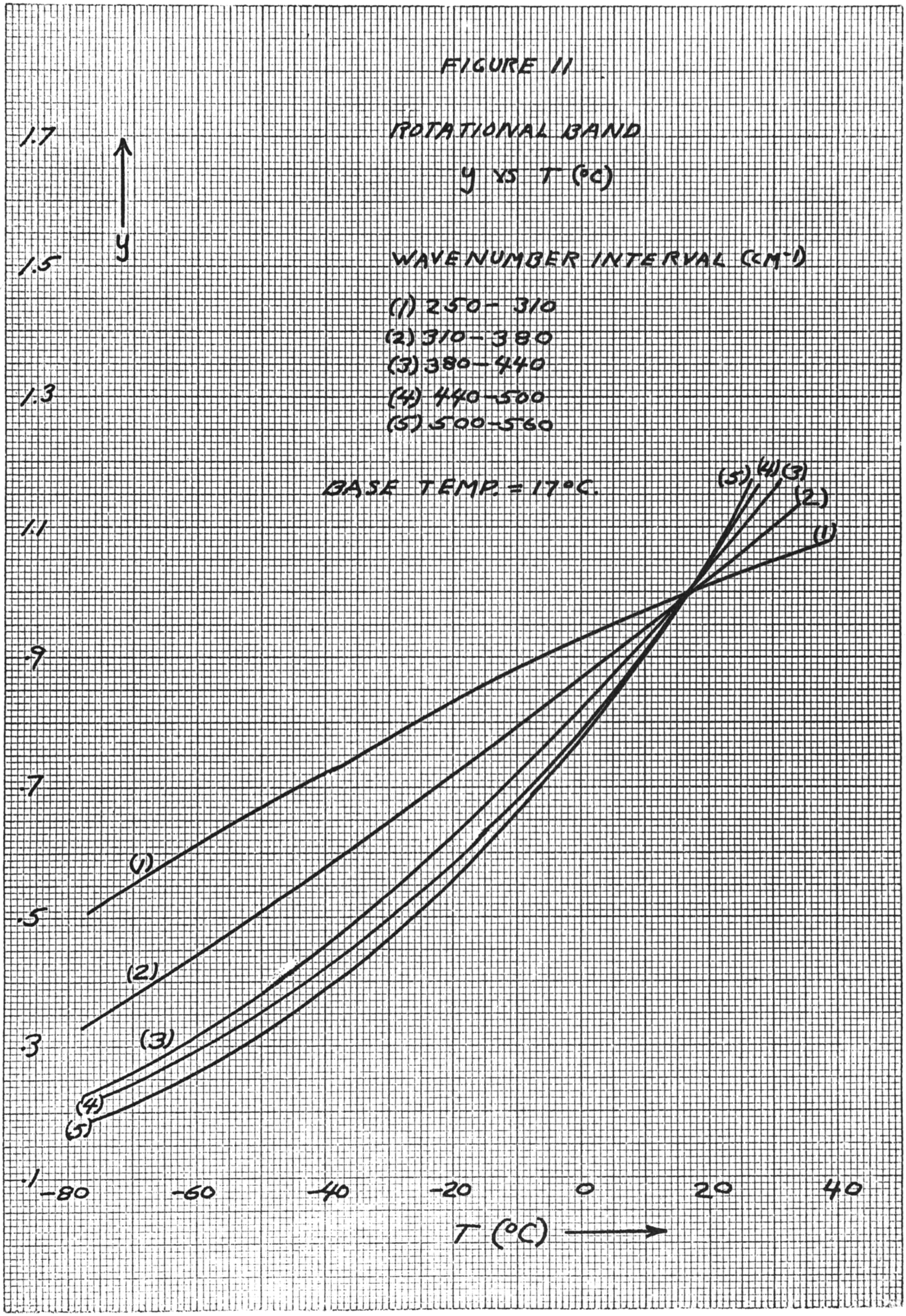
FIGURE 11
ROTATIONAL BAND
y vs T (°C)
WAVENUMBER INTERVAL (CM⁻¹)
(1) 250 – 310
(2) 310 – 380
(3) 380 – 440
(4) 440 – 500
(5) 500 – 560
BASE TEMP. = 17°C.
y
T (°C)
1.7
1.5
1.3
1.1
.9
.7
.5
.3
.1
-80
-60
-40
-20
0
20
40
(1)
(2)
(3)
(4)
(5)

The curves of y vs T are plotted for a base temperature of 17^{o}C, but the curves of x vs T are plotted for a base temperature of 7^{o}C. Consider for a moment the curves of (x vs T):

$$x = \frac{\Sigma S_i(T)}{\Sigma S_i(7^{o})}$$

If we would like to use these same curves, but have experimental data for T = 19^{o}C, we can do the following:

$$x = \frac{\Sigma S_i(T)}{\Sigma S_i(7)} \bigg/ \frac{\Sigma S_i(19)}{\Sigma S_i(7)} = \frac{\Sigma S_i(T)}{\Sigma S_i(19)}$$

Thus, the data as given for both "x" and "y" can be used for any experimental temperatures, providing that the parameters x and y are modified correctly depending on the spectral region and the corresponding base temperatures mentioned above. These factors are listed in Table 4.

Table 4. A list of corrections to the quantities "x" and "y" required because of experimental temperature differences. "x" and "y" are temperature correction factors.

SPECTRAL INTERVAL (cm^{-1})	"x" divisor	"y" divisor
50 - 100	.95	.94
100 - 150	.98	.98
150 - 200	1.00	1.01
200 - 250	1.00	1.01
250 - 310	1.01	.97
310 - 380	1.03	.95
380 - 440	1.17	1.03
440 - 500	1.17	1.04
500 - 560	1.15	1.04
560 - 620	1.16	1.16
620 - 680	1.20	1.20

Absorption of Diffuse Radiation in Rotational Band

Thus far the transmission functions have been determined only for the transmission of a parallel beam of radiation. In the real atmosphere, the radiation from one layer to another is diffuse, so an integration of τ_I must be carried out over solid angle. The integration over azimuthal angle has already been carried out and accounts for the factor π in equation (1) and the factor of 2 in equation (18) below. The integration with respect to the zenith angle must yet be carried out.

$$\tau_f = 2\int_0^{\pi/2} \tau_I(\theta)\cos\theta\,\sin\theta\,d\theta \tag{18}$$

where τ_f is the diffuse transmission function. The functions τ_I are those listed in equations 16 and 17.

For the purpose of this integration, let $x = |\log_{10}(WP) - \alpha|$ where $W = m\sec\theta$.

Consider the case where $\alpha = \log_{10}k \leq 0$; then, $x = |\log_{10} kpm\sec\theta|$

CASE I: $\log_{10}(kpm\sec\theta) \leq 0$; So, $kpm\sec\theta \leq 1$ for $\sec\theta \leq \frac{1}{kpm}$

$x = |\log(kpm\sec\theta)| = -\log_{10}(kpm\sec\theta) = -.4343\log_e(kpm\sec\theta)$

Then, $dx = -.4343\tan\theta\,d\theta$ and $10^{-x} = kpm\sec\theta$

or $\cos\theta = kpm \times 10^{x}$

So, $\tau_f = -4.605\int \tau_I (kpm)^2 10^{2x}\,dx = -4.605(kpm)^2\int \tau_I 10^{2x}\,dx$

The limits on this integral are still to be defined.

$0 \leq \theta \leq \frac{\pi}{2}$ corresponds to $1 \leq \sec\theta \leq \infty$.

So, for Case I the limits should be $1 \leq \sec\theta \leq \frac{1}{kpm}$ or $-\log_{10}(kpm) \leq x \leq 0$.

CASE II: $\log_{10}(kpm \sec\theta) \geq 0$ so, $kpm \sec\theta \geq 1$ for $\sec\theta \geq \frac{1}{kpm}$

$$x = |\log_{10}(kpm \sec\theta)| = \log_{10}(kpm \sec\theta) \doteq .4343 \log_e(kpm \sec\theta)$$

So, $dx = .4343 \tan\theta \, d\theta$ + $10^{x} = kpm \sec\theta$ or $\cos\theta = kpm \times 10^{-x}$

And, $\tau_f = 4.605 (kpm)^2 \int \tau_I 10^{-2x} dx$

The limits on this integral are $\frac{1}{kpm} \leq \sec\theta \leq \infty$ or $0 \leq x \leq \infty$.

Thus, for $\log k \geq 0$,

$$\tau_f = 4.605 (kpm)^2 \left[\int_0^{\infty} \tau_I e^{-4.605x} dx + \int_0^{-\log_{10}(kpm)} \tau_I e^{4.605x} dx \right] \quad (19)$$

If $\log k \geq 0$, kpm should simply be replaced by $\frac{pm}{k}$ in the above.

The first integral in equation (19) can be plotted and evaluated once and for all for each of the pressures used in the determination of equations (16) and (17). This curve is plotted in Fig. (12) for the high pressure region (p = 60 cm of Hg) and has been planimetered, its area being .01225. The low pressure curve has similarly been planimetered, its area being .01110. This curve appears in Fig. (13). The second integral of equation (19) has been evaluated by Simpson's Rule, and values of τ_f are tabulated as a function of $-\log_{10} kpm$ below in Table 5.

Table 5. Diffuse transmission as a function of $-\log_{10} kpm$

$\tau_f\ (p=0)$	$\tau_f\ (p=60\,cm)$	$-\log_{10} kpm$
.0745	.0829	.50
.2217	.2602	1.00
.4278	.4928	1.50
.6271	.6968	2.00
.7731	.8395	2.50
.8649	.9229	3.00
.9185	.9694	3.50
.9496	.9943	4.00
.9679	.9993	4.50
.9789	.9998	5.00

The first integral in equation (19) is so small that it is of no importance for values of $-\log_{10} kpm > 1$.

It is of interest at this point to make a comparison between the curves of beam and slab transmission for corresponding pressures. The graphs comparing the two are found in Figs. (6) and (7). A factor ranging between 1 and 2 times the actual mass will make τ_I coincide with τ_f. Thus, Elsasser's value of 1.66 might be used with reasonable accuracy to convert τ_I to τ_f through most of the region of interest. In fact, in order to obtain a basis of comparison, 1.66 m has been used in place of m to convert τ_I into τ_f (See Elsasser (1942)).

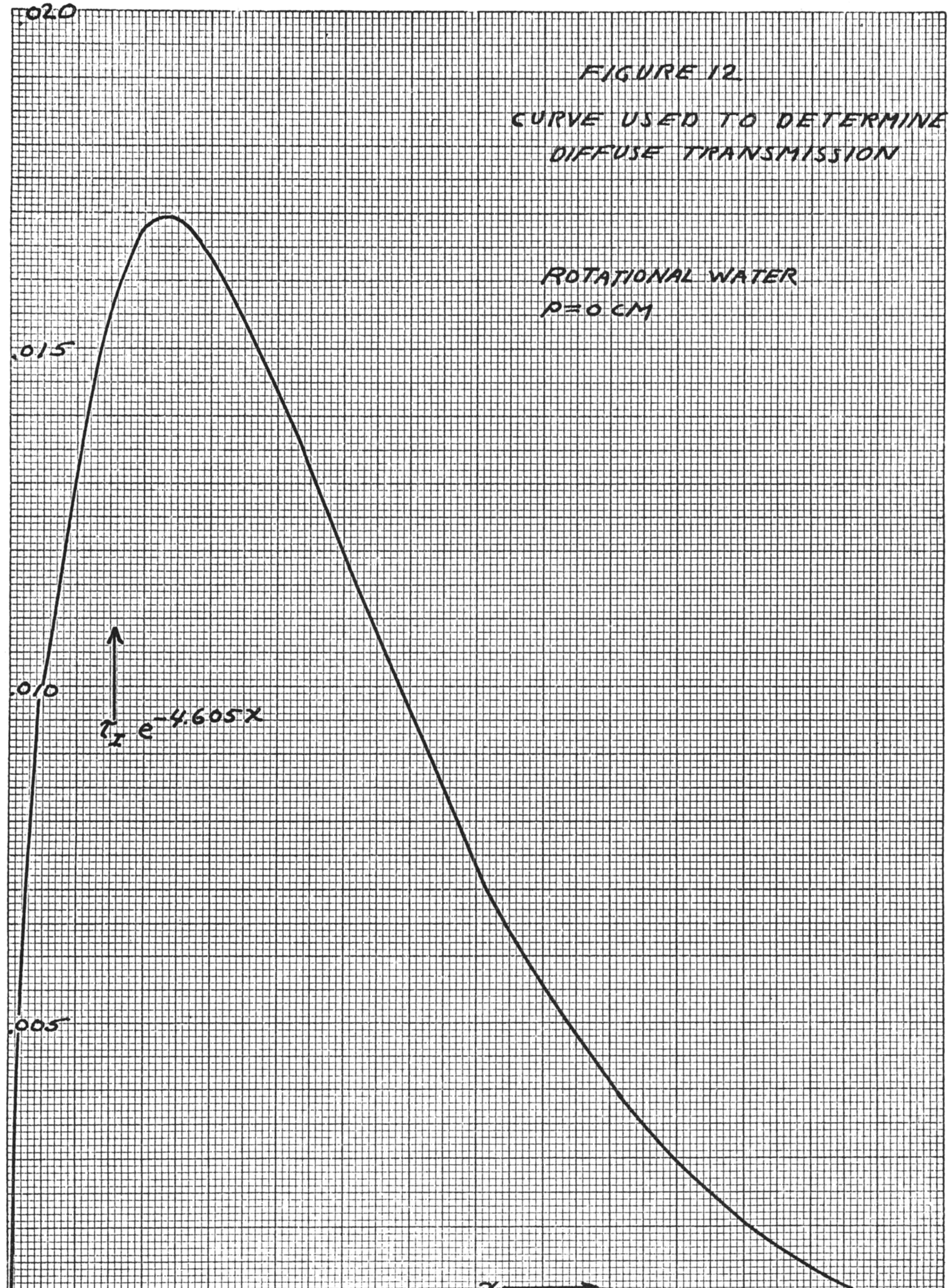
.020
.015
.010
.005
0
.5
1.0
FIGURE 12
CURVE USED TO DETERMINE
DIFFUSE TRANSMISSION
ROTATIONAL WATER
P=0 CM
$\tau_I e^{-4.605x}$
x

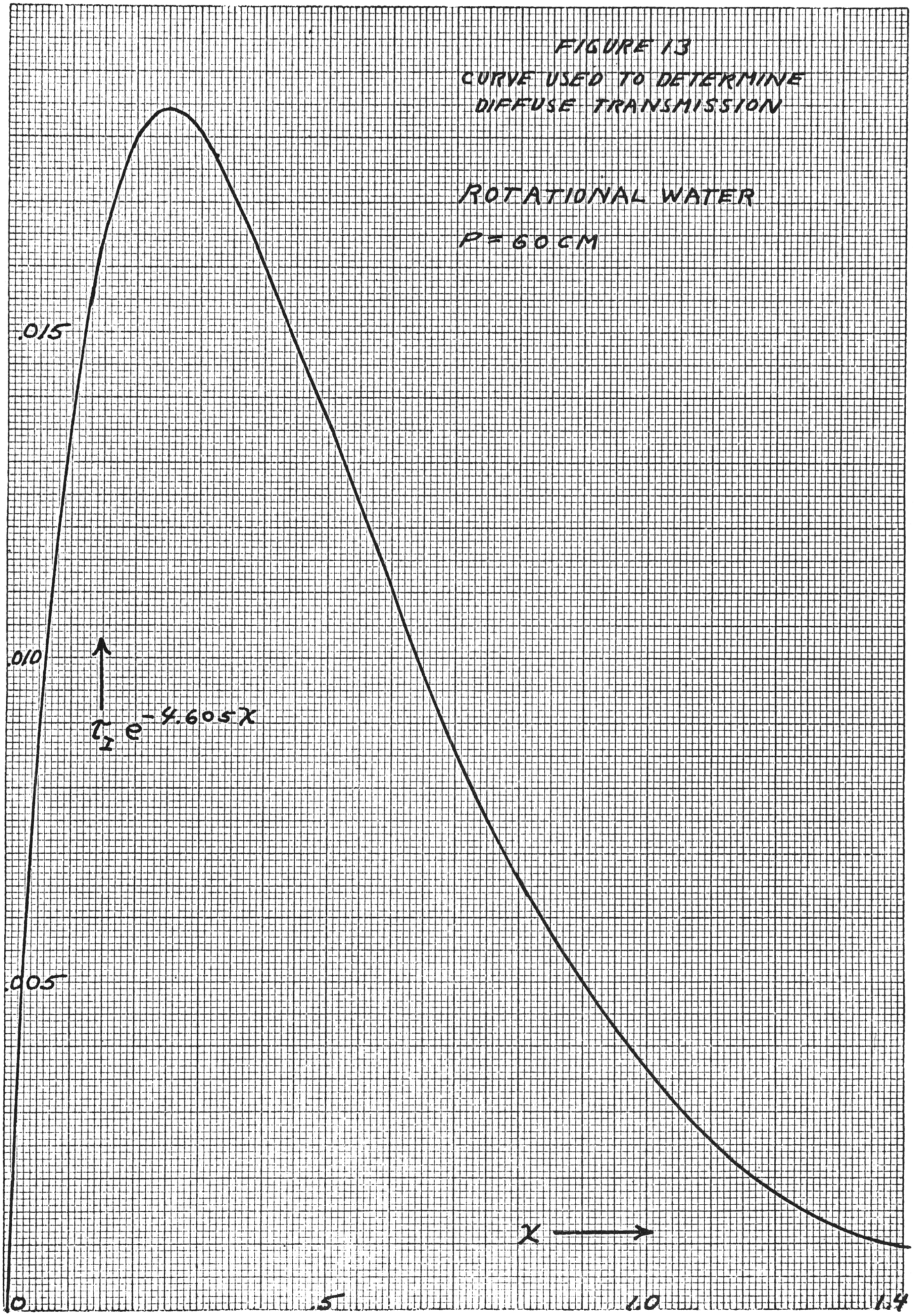
FIGURE 13
CURVE USED TO DETERMINE
DIFFUSE TRANSMISSION
ROTATIONAL WATER
P = 60 CM
.015
.010
.005
$\tau_I e^{-4.605\chi}$
χ
0
.5
1.0
1.4

V. THE 6.3-MICRON BAND

Howard, Burch and Williams (1955) have experimentally measured the transmission of radiation through various amounts of water vapor at different total pressures in the 6.3-micron water vapor band. All of their data were taken at 22°C. Their data show a remarkable fit throughout the entire range to a transmission function proposed by Goody (1952) which follows:

$$\tau_I = \exp\left[\frac{-\frac{w}{w_o}\,1.97}{\left(1+\gamma\frac{w}{w_o}\right)^{1/2}}\right] \tag{20}$$

where w_o = mass of H_2O for $\tau = .5$, γ = 6.57 for a pressure of 740 mm Hg and γ = 39.9 for a pressure of 125 mm Hg. By means of a multiplication of w/w_o by the proper value of w_o, depending on the spectral interval and division by either 740 or 125, equation 20 takes the general form:

$$\tau_I = \exp\left[\frac{-AWP}{(1+BWP)^{1/2}}\right], \quad \tau_I = \exp\left[\frac{-CWP}{(1+DWP)^{1/2}}\right] \tag{21}$$

where A and B are the high pressure (740 mm Hg) coefficients and C and D are the low pressure (125 mm Hg) coefficients. Table 6 gives the values of A, B, C, and D as a function of spectral interval.

The 6.3-micron band is effectively two displaced rotational bands either side of 1595 cm^{-1}, one of which is inverted. The same temperature correction routine can be used here as in the rotational band to determine x and y as a function of temperature for a given spectral interval. However, the line intensities (S_i) must be modified by a factor

$$\frac{1 - exp\left(-\frac{1.4388\nu}{T_0}\right)}{1 - exp\left(-\frac{1.4388\nu}{T}\right)}$$ (See Wexler (1960) and Johnson (1954)).

This has been done and the resulting curves are to be found in Figs. (15) and (16). Analytic functions have been determined to describe these curves and these expressions follow in Table 7.

Table 6. Constants used in equation (21)

wave number	A	B	C	D
1200 - 1250	1.517	5.059	48.05	973.2
1250 - 1300	.405	1.349	14.41	292.0
1300 - 1350	.1214	.4047	2.162	43.79
1350 - 1400	.0364	.1214	.721	14.60
1400 - 1450	.0091	.0304	.216	4.379
1450 - 1500	.0036	.0121	.084	1.703
1500 - 1550	.0050	.0169	.204	4.136
1550 - 1600	.0172	.057	.480	9.732
1600 - 1650	.0044	.0148	.132	2.676
1650 - 1700	.0051	.0169	.216	4.379
1700 - 1750	.0152	.0506	.541	10.950
1750 - 1800	.0465	.1551	1.562	29.200
1800 - 1850	.1739	.5801	4.204	85.15
1850 - 1900	.4652	1.551	9.610	194.6
1900 - 1950	1.214	4.047	26.43	535.2
1950 - 2000	2.629	8.769	84.09	1703.0

The resulting curve for 1250 - 1300 cm^{-1} is shown in Fig. (14) as a typical curve generated by equation(21) and Table (6).

TABLE 7

6.3-MICRON TEMPERATURE CORRECTION

WAVENUMBER INTERVAL (cm^{-1})	"X" CORRECTION $T = °K$	"Y" CORRECTION $T = °K$
1550-1600 & 1600-1650	$x = 20.01(T)^{-.5253}$	$y = 2.2036 \times 10^{2}(T)^{-.9487}$
1500-1550 & 1650-1700	$x = 20.01(T)^{-.5253}$	$y = 16.84(T)^{-.4965}$
1450-1500 & 1700-1750	$x = .6035(T)^{.0885}$	$y = .1396(T)^{.3462}$
1400-1450 & 1750-1800	$x = 5.328 \times 10^{-2}(T)^{.5141}$	$y = 3.166 \times 10^{-3}(T)^{1.012}$
1350-1400 & 1800-1850	$x = .0250(T)^{.6467}$	$y = 1.337 \times 10^{-2}(T)^{.7587}$
1300-1350 & 1850-1900	$x = 1.114 \times 10^{-4}(T)^{1.5959}$	$y = 5.385 \times 10^{-3}(T) - .589$
1250-1300 & 1900-1950	$x = 1.299 \times 10^{-7}(T)^{2.785}$	$y = 6.173 \times 10^{-7}(T)^{2.514}$
1200-1250 & 1950-2000	$x = 5.790 \times 10^{-11}(T)^{4.135}$	$y = 3.672 \times 10^{-10}(T)^{3.825}$

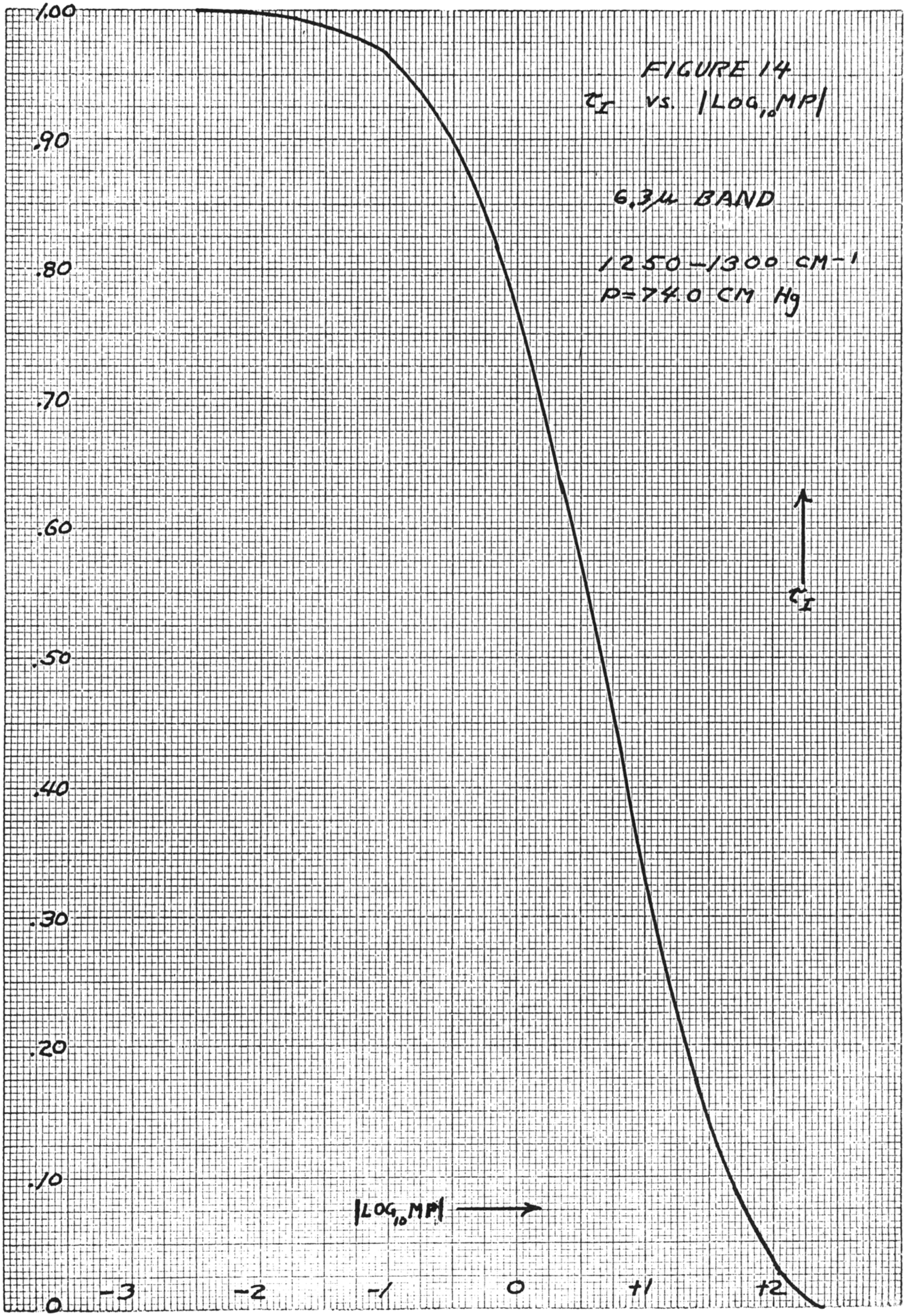
FIGURE 14
τ_I vs. $|\log_{10} MP|$
6.3μ BAND
1250–1300 CM^{-1}
P=74.0 CM Hg
1.00
.90
.80
.70
.60
.50
.40
.30
.20
.10
0
-3
-2
-1
0
+1
+2
$|\log_{10} MP|$
τ_I

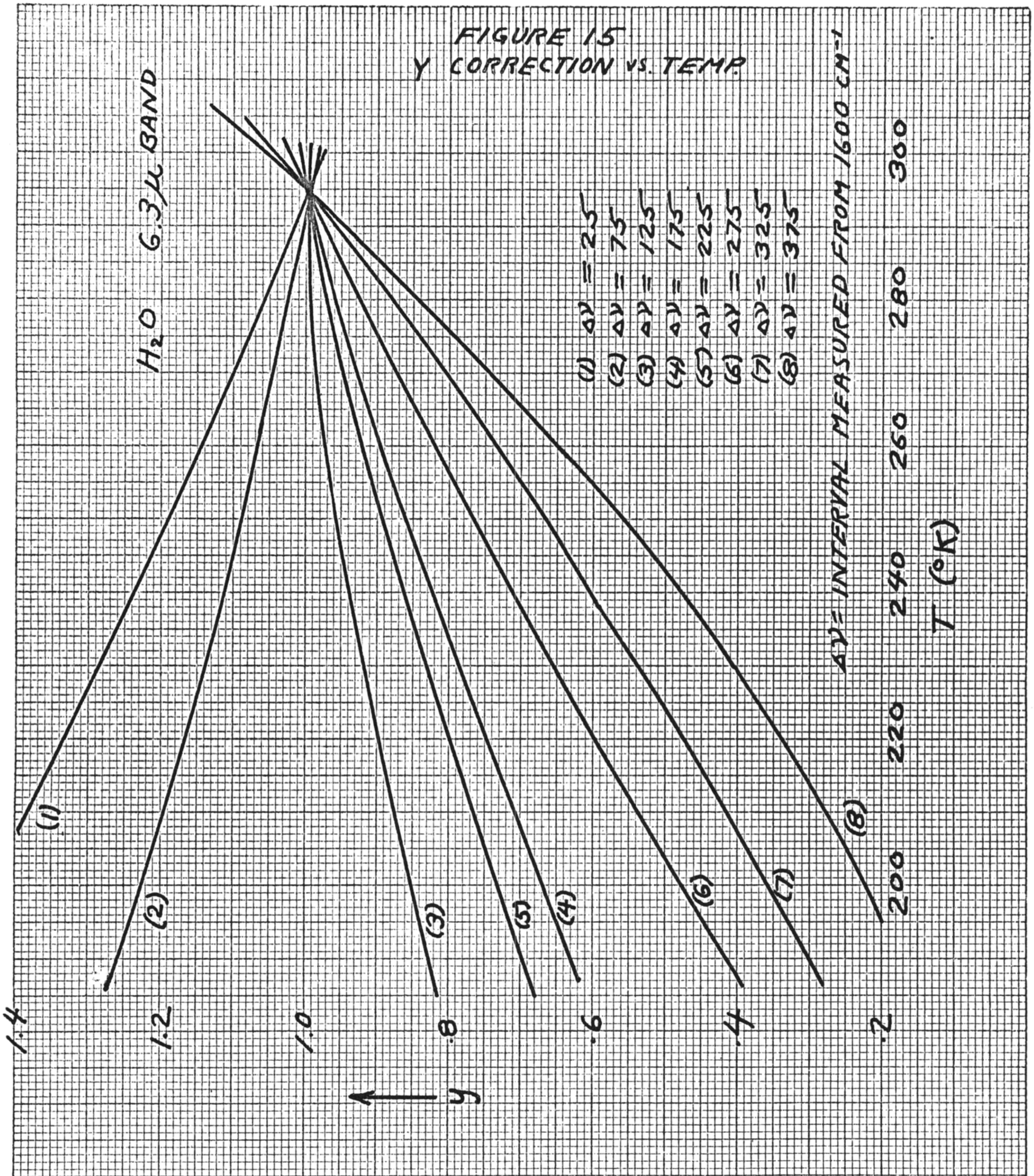

FIGURE 15
Y CORRECTION VS. TEMP.

FIGURE 16

X CORRECTION vs. TEMP.

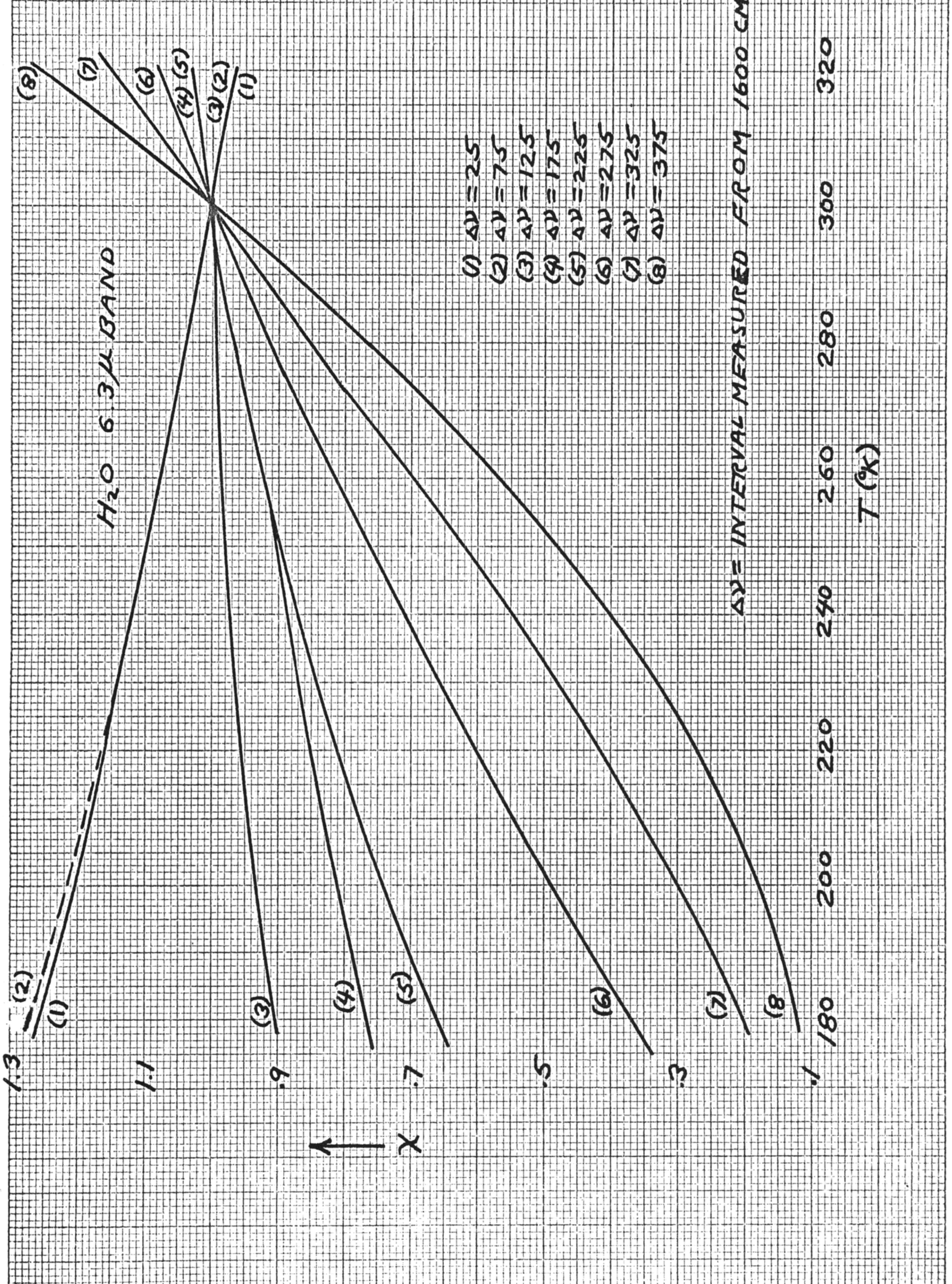

The "y" correction is valid at the experimental temperature of $22^{\circ}C$, but the "x" correction is valid at $27^{\circ}C$, so a factor must be divided into the "x" results as listed in Table 8 in order to determine the proper temperature correction factor. This is necessary because the experimental data were determined at a temperature of $22^{\circ}C$. This factor is determined in the same way as shown on page (28) for the rotational band.

Table 8. Correction to the quantity "x" resulting from the differences in experimental temperatures.

Spectral Interval	"x" divisor
1550-1600 and 1600-1650	.94
1500-1550 and 1650-1700	.96
1450-1550 and 1700-1750	.98
1400-1450 and 1750-1800	.99
1350-1400 and 1800-1850	.99
1300-1350 and 1850-1900	1.00
1250-1300 and 1900-1950	1.01
1200-1250 and 1950-1900	1.01

The only other item necessary to solve equations 9' and 10' for 6.3-micron water vapor is the integration of the function τ_I over zenith angle. Due to the relative inaccuracy of the data being used here, there will be no additional loss in accuracy by simply allowing m to become 1.66 m as was originally proposed by Elsasser (1942).

VI. RESULTS AND CONCLUSIONS

In order to obtain realistic results, three actual soundings were taken from Northern Hemisphere Data Tabulations. An attempt was made to obtain a dry, cold sounding as well as a warm, humid one. The sounding originally used by Elsasser (1942) for some of his radiation calculations was also included. The four soundings used appear in Table 9.

The computer program was written so that a cloud cover could be introduced at any level or so that clear conditions could be assumed. Each of the four soundings was used, first with clear conditions and then with a cloud cover at the top of the sounding. The flux divergence obtained from the program, and the corresponding time rates of change of temperature are listed in Tables 10, 11 and 12. Table 10 lists the flux divergence due only to the rotational band; Table 11 similarly lists the flux divergence due to the 6.3-micron band; and Table 12 lists the totals. In these three tables, $\frac{\partial T}{\partial t} = 8.467 \times 10^{-4} \frac{\Delta R}{\Delta p}$ where R is in cgs units, p is in mb, and $\frac{\partial T}{\partial t}$ is in °C/day. Table 10 also compares the results obtained for the rotational band using the transmission function found by integration over zenith angle with the results obtained with approximate procedure of using the beam transmission with 1.66 times the actual mass of water vapor. It is seen here that the difference in the flux divergence is 2% or less for most of the cases. Thus, the use of the beam transmission with 1.66 times the mass is again well justified.

In order to obtain a basis of comparison for these results, the net

Table 9. Soundings used for radiation calculations.

P (mb)	T ($^{\circ}$C)	W(pr. cm) ±.004
	Sounding No. 1	
1015	10	1.815
950	7	1.405
920	7	1.240
790	-1	.642
740	-4	.462
710	-2	.375
650	-8	.261
580	-14	.177
505	-16	.107
470	-18	.070
350	-34	.010
300	-44	.000
	Sounding No. 2	
973	28.9	4.415
933	26.3	3.892
900	26.0	3.494
850	22.8	2.899
700	11.9	1.450
500	-6.0	.302
442	-11.3	.118
400	-14.8	.047
300	-30.9	.005
250	-41.8	.000
	Sounding No. 3	
1015	29.4	5.769
1000	28.1	5.514
919	21.3	4.244
850	17.6	3.319
700	8.5	1.427
555	-2.4	.281
500	-7.4	.153
400	-19.1	.038
300	-35.2	.003
250	-44.6	.000

Table 9 (continued)

P (mb)	T ($^{\circ}$C)	W(pr. cm) $\pm$.004
	Sounding No. 4	
991	-3.2	.770
956	-3.2	.694
942	1.7	.660
926	2.9	.615
850	-1.9	.436
700	-14.3	.175
500	-32.5	.013
444	-39.7	.003
400	-45.8	.000

Sounding No. 1 Taken from p. 27 of Elsasser's 1942 Radiation Paper. (See Ref. 4)

Sounding No. 2 Taken from Northern Hemisphere Data Tabulations of July 29, 1955 for Phoenix, Arizona.

Sounding No. 3 Taken from Northern Hemisphere Data Tabulations of July 29, 1955 for Miami, Florida.

Sounding No. 4 Taken from Northern Hemisphere Data Tabulations of January 26, 1958 for Anchorage, Alaska.

Table 10. Temperature change due to flux divergence in the Rotational Band. $\partial T/\partial t = -8.467 \times 10^{-4} (\Delta R/\Delta p)$, where p is in mb and R is in ergs/cm^2/sec and $\partial T/\partial t$ is in °C/day.

Level	Δp (mb)	Factor of 1.66 used: Flux Div. (cgs units)	Factor of 1.66 used: $\partial T/\partial t$ (°C/day)	τ_f Used instead of 1.66: Flux div. (cgs units)	τ_f Used instead of 1.66: $\partial T/\partial t$ (°C/day)
		Sounding 1 - With no cloud cover			
1-2	65	4187	-.545	4160	-.542
2-3	30	2056	-.580	2144	-.605
3-4	130	11664	-.760	11632	-.758
4-5	50	6141	-1.040	6083	-1.030
5-6	30	4714	-1.330	4557	-1.286
6-7	60	8145	-1.149	7935	-1.120
7-8	70	6854	- .829	7082	- .857
8-9	75	8818	- .995	8465	- .956
9-10	35	7257	-1.756	7283	-1.762
10-11	120	25131	-1.773	24738	-1.745
11-12	50	33051	-5.597	33048	-5.596
		Sounding 1 - With cloud cover at top			
1-2	65	2261	-.295	2258	-.294
2-3	30	1073	-.303	1096	-.309
3-4	130	5424	-.353	5372	-.350
4-5	50	2478	-.420	2424	-.410
5-6	30	2078	-.586	2028	-.572
6-7	60	3392	-.479	3321	-.469
7-8	70	1980	-.239	2005	-.243
8-9	75	2151	-.243	2059	-.232
9-10	35	1738	-.420	1719	-.242
10-11	120	2091	-.148	2050	-.145
11-12	50	-318	+.054	-308	+.052

Table 10 (continued)

Sounding 2 - With no cloud cover

1-2	40	1797	-.380	1743	-.343
2-3	33	1453	-.373	1486	-.381
3-4	50	2626	-.445	2880	-.488
4-5	150	10690	-.603	10893	-.615
5-6	200	26850	-1.137	26373	-1.117
6-7	58	16828	-2.457	16705	-2.439
7-8	42	16191	-3.264	16608	-3.348
8-9	100	29258	-2.477	28850	-2.443
9-10	50	26020	-4.406	26132	-4.425

Sounding 2 - With could cover at the top

1-2	40	1169	-.247	1143	-.242
2-3	33	887	-.228	917	-.235
3-4	50	1580	-.268	1704	-.289
4-5	150	5424	-.306	5483	-.309
5-6	200	10062	-.426	9846	-.417
6-7	58	5348	-.781	5275	-.770
7-8	42	4252	-.857	4173	-.841
8-9	100	2896	-.245	2847	-.241
9-10	50	-199	+.034	-200	+.034

Sounding 3 - No cloud cover

1-2	15	654	-.369	634	-.358
2-3	81	2818	-.295	2956	-.309
3-4	69	2618	-.321	2530	-.310
4-5	150	11176	-.631	10842	-.612
5-6	145	28434	-1.660	28911	-1.688
6-7	55	12368	-1.904	12287	-1.892
7-8	100	23275	-1.971	23598	-1.998
8-9	100	29593	-2.506	30102	-2.549
9-10	50	20950	-3.548	20777	-3.518

Table 10 (concluded)

Sounding 3 - Cloud cover at top

1-2	15	482	-.272	473	-.267
2-3	81	1742	-.182	1813	-.190
3-4	69	1424	-.175	1378	-.169
4-5	150	5653	-.319	5514	-.311
5-6	145	12460	-.728	12720	-.743
6-7	55	4729	-.728	4751	-.731
7-8	100	5912	-.501	6039	-.511
8-9	100	2552	-.216	2587	-.219
9-10	50	-146	+.025	-144	+.024

Sounding 4 - No cloud cover

1-2	35	830	-.201	876	-.212
2-3	14	974	-.589	964	-.583
3-4	16	2426	-1.284	2420	-1.281
4-5	76	8791	-.979	8804	-.981
5-6	150	17168	-.969	17433	-.984
6-7	200	34024	-1.440	34354	-1.454
7-8	56	15469	-2.339	15781	-2.386
8-9	44	23002	-4.426	22910	-4.409

Sounding 4 - Cloud cover at top

1-2	35	-110	+.027	-96	+.023
2-3	14	470	-.284	469	-.284
3-4	16	1665	-.881	1681	-.890
4-5	76	4842	-.539	4906	-.547
5-6	150	5988	-.338	6091	-.344
6-7	200	4605	-.195	4664	-.197
7-8	56	794	-.120	812	-.123
8-9	44	-217	+.042	-222	+.043

Table 11. Rate of change of temperature due to flux divergence in the 6.3μ H_2O band. (factor of 1.66 used throughout)

		No Cloud Cover		Cloud Cover at Top	
Level	Δp (mb)	Flux Div. (cgs units)	$\partial T/\partial t$ ($^\circ$C/day)	Flux Div. (cgs units)	$\partial T/\partial t$ ($^\circ$C/day)
			Sounding No. 1		
1-2	65	934.8	-.122	759.2	-.099
2-3	30	379.9	-.107	297.6	-.084
3-4	130	1453.8	-.095	1061.0	-.069
4-5	50	418.7	-.071	253.9	-.043
5-6	30	278.2	-.079	182.1	-.051
6-7	60	405.9	-.057	255.3	-.036
7-8	70	182.4	-.022	47.6	-.006
8-9	75	140.9	-.016	-3.98	-.0004
9-10	35	110.6	-.027	10.35	-.003
10-11	120	143.5	-.010	111.5	-.008
11-12	50	36.7	-.006	58.7	-.010
			Sounding No. 2		
1-2	40	1028.6	-.218	907.6	-.192
2-3	33	728.4	-.187	625.1	-.160
3-4	50	1141.5	-.193	963.4	-.163
4-5	150	2440.6	-.138	1816.9	-.103
5-6	200	2084.1	-.088	1025.5	-.043
6-7	58	635.6	-.093	259.4	-.038
7-8	42	365.1	-.074	131.2	-.026
8-9	100	200.4	-.017	-31.5	+.003
9-10	50	28.3	-.005	-32.4	+.005

Table 11 (continued)

Level	Δp (mb)	No Cloud Cover: Flux Div. (cgs units)	No Cloud Cover: $\partial T/\partial t$ (^{o}C/day)	Cloud Cover at Top: Flux Div. (cgs units)	Cloud Cover at Top: $\partial T/\partial t$ (^{o}C/day)
Sounding No. 3					
1-2	15	486.9	-.275	446.2	-.252
2-3	81	1722.5	-.180	1490.9	-.156
3-4	69	901.4	-.111	689.5	-.085
4-5	150	2328.2	-.131	1649.4	-.093
5-6	145	2729.5	-.159	1768.9	-.103
6-7	55	581.7	-.090	353.2	-.054
7-8	100	473.1	-.040	153.1	-.013
8-9	100	140.5	-.012	-65.7	+.006
9-10	50	12.9	-.002	-21.5	+.004
Sounding No. 4					
1-2	35	150.6	-.036	106.3	-.026
2-3	14	109.5	-.066	87.3	-.053
3-4	16	221.8	-.117	189.5	-.100
4-5	76	857.9	-.096	709.4	-.079
5-6	150	891.2	-.050	587.0	-.033
6-7	200	345.2	-.015	-30.5	+.001
7-8	56	44.1	-.007	-22.1	+.003
8-9	44	16.0	-.003	-16.8	+.003

Table 12. Total temperature change due to flux divergence in the 6.3 μ and rotational bands of H_2O.

Level	No Cloud Cover ($\partial T/\partial t$) °C day	Cloud Cover at Tope ($\partial T/\partial t$) °C day
	Sounding No. 1	
1-2	-.664	-.393
2-3	-.712	-.393
3-4	-.853	-.419
4-5	-1.101	-.453
5-6	-1.365	-.623
6-7	-1.177	-.505
7-8	-.879	-.249
8-9	-.972	-.232
9-10	-1.789	-.245
10-11	-1.755	-.153
11-12	-5.602	+.042
	Sounding No. 2	
1-2	-.561	-.434
2-3	-.568	-.395
3-4	-.681	-.452
4-5	-.753	-.412
5-6	-1.205	-.460
6-7	-2.532	-.808
7-8	-3.422	-.867
8-9	-2.460	-.238
9-10	-4.430	+.039
	Sounding No. 3	
1-2	-.633	-.519
2-3	-.489	-.346
3-4	-.421	-.254
4-5	-.743	-.404
5-6	-1.847	-.846
6-7	-1.982	-.785
7-8	-2.038	-.524
8-9	-2.561	-.213
9-10	-3.520	+.028

Table 12 (continued)

Level	No Cloud Cover $(\partial T/\partial t)$ °C day	Cloud Cover at Top $(\partial T/\partial t)$ °C day
	Sounding No. 4	
1–2	−.248	−.003
2–3	−.649	−.337
3–4	−1.398	−.990
4–5	−1.077	−.626
5–6	−1.034	−.377
6–7	−1.469	−.196
7–8	−2.393	−.120
8–9	−4.412	+.046

Table 13. A comparison of the use of the method reported in this paper and the method of the Elsasser Radiation Chart. All units are ergs/cm^2-sec.

According to this paper		According to Elsasser Chart	
Net upward flux $\times 10^{-4}$	Flux Div $\times 10^{-4}$	Net upward flux $\times 10^{-4}$	Flux Div $\times 10^{-4}$
5.385	.509	7.839	.677
5.894	.253	8.516	.230
6.147	1.308	8.746	2.290
7.455	.651	11.036	.217
8.106	.484	11.253	.632
8.589	.834	11.885	1.131
9.423	.726	13.016	.337
10.150	.861	13.353	.868
11.010	.739	14.221	.872
11.750	2.488	15.093	2.279
14.238	3.308	17.372	7.223
17.546		24.595	

upward flux corresponding to Sounding No. 1 has been determined through the use of the Elsasser Diagram (Elsasser (1942)) and Johnson (1954). Table 13 lists both the net upward flux and the flux divergence as determined by the method of this paper and according to Elsasser's radiation chart. Although the agreement is not too good, it is seen that the variation of the flux divergence is similar.

It is also interesting here to notice the large values of flux divergence obtained toward the top of the sounding - particularly in the top layer itself. According to Table 12, this corresponds to the large rate of change of temperature of -5.6°C/day. The Elsasser diagram would yield an even larger temperature decrease. Either there is very strong cooling at this level or an explanation must be found that will explain the similar results predicted by both techniques.

The sounding data themselves permit an uncertainty in the mass of precipitable water of 0.004 cm. Thus, it is possible that between 300 mb and the top of the atmosphere there may be as much as .004 cm of precipitable water. The only reason that a zero is entered in the sounding at 300 mb is that the instrument could no longer measure the amount of water vapor present. In fact, at a temperature of -44°C, the humidity sensor of a radiosonde is inactive below a relative humidity of about 20%. This humidity would correspond to a mixing ratio at 300 mb of .05 rather than zero. Based on a standard atmosphere between 200 and 300 mb (Wexler 1959), an average mixing ratio of .026 might be assumed. Thus, an amount of precipitable water of .003 cm between these levels might be present to contribute substantially to the downward radiation flux at 300 mb. By assuming the slightly worse case of .004 cm of water between 200 mb and 300 mb, the net upward flux at 300 mb was determined on the Elsasser diagram. The net upward flux at 300 mb would then be 18.135×10^4 instead of 24.595×10^4, indicating a flux divergence between 300 and 350 mb of only .763. The influence of this .004 cm of water on the net upward flux at 350 mb would be much less - the flux there would be 16.895×10^4 instead of 17.372×10^4 yielding a flux divergence between 470 mb and 350 mb of 1.802. Thus, the flux divergence here is only altered by about 20%. The levels below this will be almost unaffected by such an inaccuracy in measuring the amount of absorber.

Thus, the computed flux divergence in the top layer should be discarded, and in the second layer from the top the results should be considered with the knowledge of the maximum error. In a typical case the error in the next-to-top layer would be expected to be considerably smaller than the maximum. In order to determine more accurate values at the top of such a sounding, the assumption of a standard atmosphere above the "top" level will substantially decrease the error in the "top" levels. In order to demonstrate this more clearly, the Elsasser sounding has been run with an additional point in the sounding at 200 mb. This has been done such that the level between 300 and 200 mb contains .004 cm of precipitable water, the rest of the sounding remaining the same. The results follow in Table 14. The percent change in the quantity ($\partial T/\partial t$) may be taken as a measure of the error introduced in the "top" layers by the inability to measure the water vapor more accurately.

Table 14. An estimate of the error introduced into the calculations by inability to measure small amounts of water vapor at high levels.

Level	Net Upward Flux Total Both Bands (cgs units)	Layer	Flux Div. (ergs/cm^2-sec)	($\partial T/\partial t$) (°C day)	% Error
1	53851.27	1-2	5095.79	-.664	0
2	58947.06	2-3	2524.98	-.713	0
3	61472.04	3-4	13091.96	-.853	0
4	74564.00	4-5	6507.55	-1.102	0
5	81071.55	5-6	4840.77	-1.366	0
6	85912.32	6-7	8353.95	-1.179	0
7	94266.27	7-8	7289.85	-.882	0.3
8	101556.12	8-9	8659.61	-.978	0.6
9	110215.73	9-10	7469.36	-1.807	1.0
10	117685.09	10-11	26334.56	-1.858	5.9
11	114019.65	11-12	36050.37	-3.605	36.0
12	153735.46				

With the exception of the new "top" layer the results here stated should be quite satisfactory within the accuracy of both the experimentally determined transmission functions and the soundings themselves.

Before going further with this technique, actual measurements of flux divergence accompanied by complete soundings to high levels are needed. Then the validity of the method could be tested and compared with experiment.

In addition to the problem of obtaining accurate soundings, this method is limited by the experimentally determined transmission functions. To this extent the method should give quite accurate results. By employing this technique to various atmospheric soundings, a person might better be able to understand the physical process and resulting cooling rate due to radiative heat transfer in the atmosphere.

APPENDIX I

The purpose of this appendix is to display the actual Computer programs used for this report. The programs are written in FORTRAN for use on the IBM 709 Computer.

A description of the variables used in the program follows:

Actual Variable	Fortran Variable
$m_e p_e$	EMP
m_e	EM
τ (high pressure)	TAUH
τ (low pressure)	TAUL
τ (value actually used)	TAW
x	X
y	Y
B	BLAK
T (^{o}K)	TA
T (^{o}C) (average for a layer)	AT
p (atm) (average for a layer)	AP
p_e	PA
ΔB	BLAK
R	SUM

Copies of the actual programs and data used appear in the following pages.

ROTATIONAL BAND

```
*M1596-1103, FMS, RESULT, 10,12, 5000, 0,               MCCLATCHEY THESIS
*     XEQ
*     LIST
      DIMENSION QNU(11), DELTNU(11), ALPHA(11), T(50), P(50), W(50),
     1AX(11), BX(11), CX(11), DX(11), EX(11), AY(11), BY(11), CY(11),
     2DY(11), EY(11), TA(50), AT(50), AP(50), DELTAM(50), BLAK(11, 50)
      IF DIVIDE CHECK 441, 441
  441 READ INPUT TAPE 4, 202, (AX(L), L=1,11)
      READ INPUT TAPE 4, 214, (BX(L), L=1,11), (BY(L), L=1,11)
      READ INPUT TAPE 4, 216, (CX(L), L=1,11), (CY(L), L=1,11)
      READ INPUT TAPE 4, 218, (DX(L), L=1,11)
      READ INPUT TAPE 4, 204, (EX(L), L=1,11)
      READ INPUT TAPE 4, 222, (AY(L), L=1,11)
      READ INPUT TAPE 4, 226, (DY(L), L=1,11)
      READ INPUT TAPE 4, 204, (EY(L), L=1,11)
  450 READ INPUT TAPE 4, 195, (QNU(L), L=1,11)
      READ INPUT TAPE 4, 208, (DELTNU(L), L=1,11)
      READ INPUT TAPE 4, 210, (ALPHA(L), L=1,11)
  500 READ INPUT TAPE 4, 206, NI, NOC
  502 READ INPUT TAPE 4, 200, (T(J), J=1,NI)
      READ INPUT TAPE 4, 202, (P(J), J=1, NI)
      READ INPUT TAPE 4, 202, (W(J), J=1, NI)
      DO 7 J=1, NI
      TA(J)=T(J)+273.
      AT(J)=(T(J)+T(J+1))/2.
      AP(J)=(P(J)+P(J+1))/2.
      DELTAM(J)=(W(J)-W(J+1))
    7 CONTINUE
      DO 11 L=1,11
      DO 9 J=1,NI
      BLAK(L,J)=.00001190605*QNU(L)**3./(EXPF(1.43868*QNU(L)/TA(J))-1.)
    9 CONTINUE
   11 CONTINUE
      DO 92 N=1, NI
      SUM=0
   12 DO 80 L=1,11
      SUMX = 0.
      SUMY = 0.
      SUMZ = 0.
      I=NI-1
      DO 60 K=1,I
      IF (K-N) 13, 14, 15
   13 J=N-K
      GO TO 298
   14 SUMX = 0.
      SUMY = 0.
   15 J=K
  298 IF (L-4) 299, 300, 300
  299 X=(AX(L)+BX(L)*(AT(J)+CX(L))**DX(L))/EX(L)
      Y=(AY(L)+BY(L)*(AT(J)+CY(L))**DY(L))/EY(L)
      GO TO 17
  300 IF (L-7) 301, 302, 302
  301 X=(AX(L)+BX(L)*COSF((AT(J)+CX(L))/DX(L)))/EX(L)
      Y=(AY(L)+BY(L)*COSF((AT(J)+CY(L))/DY(L)))/EY(L)
      GO TO 17
  302 IF (L-10) 303, 299, 299
  303 X=(AX(L)+BX(L)*(AT(J)+CX(L))**DX(L))/EX(L)
      Y=(AY(L)+BY(L)*COSF((AT(J)+CY(L))/DY(L)))/EY(L)
   17 EMP=Y*AP(J)*DELTAM(J)
```

ROTATIONAL BAND

```
                                                    2
      EM=X*DELTAM(J)
      SUMY=SUMY+EMP
      SUMX=SUMX+EM
      PA=SUMY/SUMX
      A=.4343*LOGF(SUMY)
      IF (A-ALPHA(L)) 30, 40, 40
   30 B=ABSF(A-ALPHA(L))
      IF (B-4.) 32,32,31
   31 TAUH=1.
      GO TO 33
   32 TAUH=(B**3.+1.26*B**2.+.67*B)/(B**3.+.87*B**2.+9.05)
   33 TAUL=(B**3.+.03*B**2.+.8*B)/(B**3.+.035*B**2.+7.2)
      TAW=(TAUH-TAUL)*PA/.79+TAUL
      IF (TAW-1.) 36,36,35
   35 TAW=1.
   36 GO TO 42
   40 TAW=0.
   42 DBLAK=BLAK(L,J)-BLAK(L,J+1)
      DFLUX=TAW*DBLAK*3.141593
   56 SUMZ=SUMZ+DFLUX
   60 CONTINUE
      IF (N-NI) 64, 1, 1
    1 TAW=1.
   64 IF (NOC) 70, 70, 65
   65 FTIN=TAW*BLAK(L,NI)*3.141593
      SUM=SUM+(FTIN+SUMZ)*DELTNU(L)
      GO TO 80
   70 SUM=SUM+SUMZ*DELTNU(L)
   80 CONTINUE
   90 WRITE OUTPUT TAPE 2, 100, T(1), P(1), N, SUM
   92 CONTINUE
      GO TO 500
  100 FORMAT (6H T(1)=F4.0, 6H P(1)=F6.3, 3H N=I2, 5H SUM=E14.7)
  195 FORMAT(11F5.0)
  200 FORMAT(14F5.0)
  202 FORMAT(12F6.3)
  204 FORMAT(11F5.2)
  206 FORMAT(I3,I2)
  208 FORMAT(11F4.0)
  210 FORMAT(11F6.2)
  214 FORMAT(7E10.2)
  216 FORMAT (11F6.0)
  219 FORMAT(8F8.2)
  222 FORMAT(9F7.3)
  226 FORMAT(8F9.3)
      END
*     DATA
0.000 1.608 1.000 0.000 0.000 1.200 0.000 0.170 0.100 0.000 0.000
 1.55E+03 -2.17E-03  0.00E+00  1.00E+00  1.25E+00 -1.10E+00  5.75E-10
 4.05E-05  4.72E-05  2.00E-10  3.48E-12  1.80E+03  7.70E+00  7.57E-02
 1.02E+00  1.28E+00  0.62E+00 -1.00E+00 -0.95E+00 -0.90E+00  2.29E-10
 5.01E-12
 273.  273.  273.  -17. -115.  148.  273.  136.  132.  273.  273.
 273.  273.  273.  -40. -145. -119.  121.  102.   97.  273.  273.
  -1.30     1.00     1.00   220.00   166.00   111.30     3.77     2.00
   2.00     3.96     4.68
0.95 0.98 1.00 1.00 1.01 1.03 1.17 1.17 1.15 1.16 1.20
 0.000  0.000  0.000  0.000  0.000  0.800  1.100  1.100  1.000
```

ROTATIONAL BAND

```
                                        3
0.000  0.000
 -1.310    -0.364     0.458  167.000  191.000    81.900    93.900    80.900
  72.600     3.940     4.618
0.94 0.98 1.01 1.01 0.97 0.95 1.03 1.04 1.04 1.16 1.20
 75. 125. 175. 225. 280. 345.:410. 470. 530. 590. 650.
50. 50. 50. 50. 60. 70. 60. 60. 60. 60. 60.
-1.85 -1.92 -1.80 -1.73 -1.40  -.99  -.40  -.02   .37   .86  1.45
 3 1
 10.  -1. -14.
1.002  .780  .573
1.830 0.654 0.189
12 1
 10.   7.   7.  -1.  -4.  -2.  -8. -14. -16. -18. -34. -44.                T-1
1.002 0.938 0.908 0.780 0.731 0.701 0.642 0.573 0.499 0.464 0.346 0.296P-1
1.815 1.405 1.240 0.642 0.462 0.375 0.261 0.177 0.107 0.070 0.010 0.000W-1
12 0
 10.   7.   7.  -1.  -4.  -2.  -8. -14. -16. -18. -34. -44.                T-1C
1.002 0.938 0.908 0.780 0.731 0.701 0.642 0.573 0.499 0.464 0.346 0.296P-1C
1.815 1.405 1.240 0.642 0.462 0.375 0.261 0.177 0.107 0.070 0.010 0.000W-1C
10 1
 29.  26.  26.  23.  12.  -6. -11. -15. -31. -42.                          T-2
0.961 0.921 0.888 0.839 0.691 0.494 0.436 0.395 0.296 0.246                P-2
4.415 3.892 3.494 2.899 1.450 0.302 0.118 0.047 0.005 0.000                W-2
10 0
 29.  26.  26.  23.  12.  -6. -11. -15. -31. -42.                          T-2C
0.961 0.921 0.888 0.839 0.691 0.494 0.436 0.395 0.296 0.246                P-2C
4.415 3.892 3.494 2.899 1.450 0.302 0.118 0.047 0.005 0.000                W-2C
10 1
 29.  28.  21.  18.   9.  -2.  -7. -19. -35. -45.                          T-3
1.002 0.987 0.907 0.839 0.691 0.548 0.494 0.395 0.296 0.247                P-3
5.769 5.514 4.244 3.319 1.427 0.281 0.153 0.038 0.003 0.000                W-3
10 0
 29.  28.  21.  18.   9.  -2.  -7. -19. -35. -45.                          T-3C
1.002 0.987 0.907 0.839 0.691 0.548 0.494 0.395 0.296 0.247                P-3C
5.769 5.516 4.244 3.319 1.427 0.281 0.153 0.038 0.003 0.000                W-3C
 9 1
 -3.  -3.   2.   3.  -2. -14. -33. -40. -46.                               T-4
0.978 0.944 0.930 0.914 0.839 0.691 0.494 0.438 0.395                      P-4
0.770 0.694 0.660 0.615 0.436 0.175 0.013 0.003 0.000                      W-4
 9 0
 -3.  -3.   2.   3.  -2. -14. -33. -40. -46.                               T-4C
0.978 0.944 0.930 0.914 0.839 0.691 0.494 0.438 0.395                      P-4C
0.770 0.694 0.660 0.615 0.436 0.175 0.013 0.003 0.000                      W-4C
                                                                          160

                                                              TOTAL       160*
```

6.3-MICRON BAND

```
*M1596-1103,FMS,DEBUG,7,10,1000,0            MCCLATCHEY THESIS
*     XEQ
*     LIST
      DIMENSION QNU(16),T(50),P(50),W(50),BX(16),DX(16),EX(16),AY(16),
     1BY(16),DY(16),A(16),B(16),C(16),D(16),TA(50),AT(50),AP(50),
     2DELTAM(50),BLAK(16,50)
      IF DIVIDE CHECK 441, 441
  441 READ INPUT TAPE 4, 202, (BX(L),L=1,16)
      READ INPUT TAPE 4, 204, (DX(L),L=1,16)
      READ INPUT TAPE 4, 206, (EX(L),L=1,16)
      READ INPUT TAPE 4,208, (AY(L),L=1,16)
      READ INPUT TAPE 4,202,(BY(L),L=1,16)
      READ INPUT TAPE 4, 204, (DY(L),L=1,16)
  450 READ INPUT TAPE 4, 214, (QNU(L),L=1,16)
      READ INPUT TAPE 4, 204, (A(L),L=1,16)
      READ INPUT TAPE 4, 204, (B(L),L=1,16)
      READ INPUT TAPE 4, 222, (C(L),L=1,16)
      READ INPUT TAPE 4, 224, (D(L),L=1,16)
  500 READ INPUT TAPE 4, 226, NI, NOC
  502 READ INPUT TAPE 4, 228, (T(J),J=1,NI)
      READ INPUT TAPE 4, 208, (P(J),J=1,NI)
      READ INPUT TAPE 4, 208, (W(J),J=1,NI)
      DO 7 J=1, NI
      TA(J)=T(J)+273.
      AP(J)=(P(J)+P(J+1))/2.
      DELTAM(J)=1.66*(W(J)-W(J+1))
    7 CONTINUE
      DO 8 J=1,NI
      AT(J)=(TA(J)+TA(J+1))/2.
    8 CONTINUE
      DO 11 L=1,16
      DO 9 J=1,NI
      BLAK(L,J)=.00001190605*QNU(L)**3./(EXPF(1.43868*QNU(L)/TA(J))-1.)
    9 CONTINUE
   11 CONTINUE
      DO 92 N=1, NI
      SUM=0
   12 DO 80 L=1,16
      SUMX = 0.
      SUMY = 0.
      SUMZ = 0.
      I=NI-1
      DO 60 K=1,I
      IF (K-N) 13, 14, 15
   13 J=N-K
      GO TO 298
   14 SUMX = 0.
      SUMY = 0.
   15 J=K
  298 X=(BX(L)*AT(J)**DX(L))/EX(L)
      Y=AY(L)+BY(L)*AT(J)**DY(L)
   17 EMP=Y*AP(J)*DELTAM(J)
      EM=X*DELTAM(J)
      SUMY=SUMY+EMP
      SUMX=SUMX+EM
      PA=SUMY/SUMX
      TAUH=EXPF(-A(L)*SUMY/((1+B(L)*SUMY)**.5))
      TAUL=EXPF(-C(L)*SUMY/((1+D(L)*SUMY)**.5))
      TAW=(TAUH-TAUL)*PA/.809+TAUL
```

6.3-MICRON BAND

```
                                                    1
      IF(TAW-1.) 42,42,35
   35 TAW=1.
   42 DBLAK=BLAK(L,J)-BLAK(L,J+1)
      DFLUX=TAW*DBLAK*3.141593
   56 SUMZ=SUMZ+DFLUX
   60 CONTINUE
      IF (N-NI) 64, 1, 1
    1 TAW=1.
   64 IF (NOC) 70, 70, 65
   65 FTIN=TAW*BLAK(L,NI)*3.141593
      SUM=SUM+(FTIN+SUMZ)*50.
      GO TO 80
   70 SUM=SUM+SUMZ*50.
   80 CONTINUE
   90 WRITE OUTPUT TAPE 2, 100, T(1), P(1), N, SUM
   92 CONTINUE
      GO TO 500
  100 FORMAT (6H T(1)=F4.0, 6H P(1)=F6.3, 3H N=I2, 5H SUM=E14.7)
  202 FORMAT (7E10.3)
  204 FORMAT (10F7.4)
  206 FORMAT (14F5.2)
  208 FORMAT (12F6.3)
  214 FORMAT (12F6.0)
  222 FORMAT (10F7.3)
  224 FORMAT (9F8.3)
  226 FORMAT (I3, I2)
  228 FORMAT (14F5.0)
      END
*     DATA
5.790E-11 1.299E-07 1.114E-04 2.500E-02 5.328E-02 6.035E-01 2.001E+01
2.001E+01 2.001E+01 2.001E+01 6.035E-01 5.328E-02 2.500E-02 1.114E-04
1.299E-07 5.790E-11
4.1350 2.7850 1.5959 0.6467 0.5141 0.0885 -.5253 -.5253 -.5253 -.5253
0.0885 0.5141 0.6467 1.5959 2.7850 4.1350
0.94 0.96 0.98 0.99 0.99 1.00 1.01 1.01 1.01 1.01 1.00 0.99 0.99 0.98
0.96 0.94
0.000 0.000 -.589 0.000 0.000 0.000 0.000 0.000 0.000 0.000 0.000 0.000
0.000 -.589 0.000 0.000
3.672E-10 6.173E-07 5.385E-03 1.337E-02 3.166E-03 1.396E-01 1.684E+01
2.204E+02 2.204E+02 1.684E+01 1.396E-01 3.166E-03 1.337E-02 5.385E-03
6.173E-07 3.672E-10
3.8250 2.5140 1.0000 0.7587 1.0120 0.3462 -.4965 -.9487 -.9487 -.4965
0.3462 1.0120 0.7587 1.0000 2.5140 3.8250
1225. 1275. 1325. 1375. 1425. 1475. 1525. 1575. 1625. 1675. 1725. 1775.
1825. 1875. 1925. 1975.
1.5170 0.4045 0.1214 0.0364 0.0091 0.0036 0.0050 0.0172 0.0044 0.0051
0.0152 0.0465 0.1739 0.4652 1.2140 2.6290
5.0590 1.3490 0.4047 0.1214 0.0304 0.0121 0.0169 0.0570 0.0148 0.0169
0.0506 0.1551 0.5801 1.5510 4.0470 8.7690
48.050 14.410 02.162  0.721  0.216  0.084  0.204  0.480  0.132  0.216
 0.541  1.562  4.204  9.610 26.450 84.090
973.200 292.000  43.790  14.600   4.379   1.703   4.136   9.732   2.676
  4.379  10.950  29.200  85.150 194.600 535.2001703.000
 3 1
 10.  -1. -14.
1.002  .780  .573
1.830 0.654 0.169
12 1
```

6.3-MICRON BAND

```
 10.    7.    7.  -1.   -4.   -2.   -8. -14. -16. -18. -34. -44.              T-1
1.002 0.938 0.908 0.780 0.731 0.701 0.642 0.573 0.499 0.464 0.346 0.296P-1
1.815 1.405 1.240 0.642 0.462 0.375 0.261 0.177 0.107 0.070 0.010 0.000W-1
12 0
 10.    7.    7.  -1.   -4.   -2.   -8. -14. -16. -18. -34. -44.              T-1C
1.002 0.938 0.908 0.780 0.731 0.701 0.642 0.573 0.499 0.464 0.346 0.296P-1C
1.815 1.405 1.240 0.642 0.462 0.375 0.261 0.177 0.107 0.070 0.010 0.000W-1C
10 1
 29.   26.   26.   23.   12.   -6. -11. -15. -31. -42.                        T-2
0.961 0.921 0.888 0.839 0.691 0.494 0.436 0.395 0.296 0.246                   P-2
4.415 3.892 3.494 2.899 1.450 0.302 0.118 0.047 0.005 0.000                   W-2
10 0
 29.   26.   26.   23.   12.   -6. -11. -15. -31. -42.                        T-2C
0.961 0.921 0.888 0.839 0.691 0.494 0.436 0.395 0.296 0.246                   P-2C
4.415 3.892 3.494 2.899 1.450 0.302 0.118 0.047 0.005 0.000                   W-2C
10 1
 29.   28.   21.   18.    9.   -2.   -7. -19. -35. -45.                        T-3
1.002 0.987 0.907 0.839 0.691 0.548 0.494 0.395 0.296 0.247                   P-3
5.769 5.514 4.244 3.319 1.427 0.281 0.153 0.038 0.003 0.000                   W-3
10 0
 29.   28.   21.   18.    9.   -2.   -7. -19. -35. -45.                        T-3C
1.002 0.987 0.907 0.839 0.691 0.548 0.494 0.395 0.296 0.247                   P-3C
5.769 5.514 4.244 3.319 1.427 0.281 0.153 0.038 0.003 0.000                   W-3C
 9 1
 -3.   -3.    2.    3.   -2.  -14. -33. -40. -46.                             T-4
0.978 0.944 0.930 0.914 0.839 0.691 0.494 0.438 0.395                         P-4
0.770 0.694 0.660 0.615 0.436 0.175 0.013 0.003 0.000                         W-4
 9 0
 -3.   -3.    2.    3.   -2.  -14. -33. -40. -46.                             T-4C
0.978 0.944 0.930 0.914 0.839 0.691 0.494 0.438 0.395                         P-4C
0.770 0.694 0.660 0.615 0.436 0.175 0.013 0.003 0.000                         W-4C
                                                                             148

                                                                TOTAL       148*
```

APPENDIX II

Diermendjian (1960) proposes $\tau = \exp(-.1\ m)$ as a value which may be used for the transmission function in the window region around 10 microns. Thus, in order to determine the effect of such a transmission and to determine net upward flux and flux divergence in the entire region $50 < \nu < 2000\ cm^{-1}$, calculations of net upward flux have been made in the region from $680\text{-}1200\ cm^{-1}$ based on this above-mentioned transmission function. Elsasser's effective mass of 1.66 times the actual mass has been used to convert beam transmission to diffuse transmission.

The results of window transmission are listed in Table 15 and the rates of change of temperature for $50 < \nu < 2000\ cm^{-1}$ are listed in Table 16.

In this region there is also anomalous behavior of the top levels due to setting a zero at the top of the soundings.

Table 15. Temperature change due to flux divergence in the window region $680 < \nu < 1200$.

Level	No cloud cover Flux Div. (cgs units)	No cloud cover ∂T/∂t (°C/ day)	Cloud cover at top Flux (cgs units)	Cloud cover at top ∂T/∂t (°C/day)
Sounding No. 1				
1–2	6973.5	–.091	4524.9	–.059
2–3	2775.5	–.078	1442.1	–.041
3–4	9215.3	–.060	5223.5	–.034
4–5	2359.3	–.040	1078.1	–.018
5–6	1152.7	–.033	519.6	–.015
6–7	1408.7	–.020	565.1	–.008
7–8	717.3	–.009	127.7	–.002
8–9	488.8	–.006	–44.5	+.001
9–10	224.2	–.005	–60.2	+.001
10–11	105.9	–.001	–359.1	+.003
11–12	–12264.9	+.208	–118.6	+.002
Sounding No. 2				
1–2	8297.6	–.176	6149.0	–.130
2–3	6351.2	–.163	4586.5	–.118
3–4	9702.2	–.164	6836.7	–.116
4–5	21413.1	–.121	13128.0	–.074
5–6	11831.7	–.050	3696.1	–.016
6–7	1092.5	–.016	–361.8	+.005
7–8	271.8	–.005	–301.4	+.006
8–9	–49.0	–.000	–391.2	+.003
9–10	–25647.5	+.434	–78.3	+.001

Table 15 (continued)

Sounding No. 3

1-2	3524.2	-.199	2763.1	-.156
2-3	16050.7	-.168	11741.0	-.123
3-4	11019.5	-.135	7256.4	-.089
4-5	23513.8	-.133	13759.0	-.078
5-6	13331.4	-.078	5748.0	-.034
6-7	1171.5	-.018	231.4	-.004
7-8	532.0	-.005	-329.8	0
8-9	-83.4	+.001	-349.0	+.003
9-10	-28287.1	+.479	-47.3	+.001

Sounding No. 4

1-2	1230.5	-.030	730.5	-.018
2-3	612.3	-.037	386.5	-.023
3-4	905.9	-.048	605.1	-.032
4-5	3422.0	-.038	2203.2	-.025
5-6	3774.4	-.021	1930.9	-.011
6-7	4858.6	-.021	-100.8	.000
7-8	6.9	.000	-67.2	+.001
8-9	-5376.0	+.103	-28.0	+.001

Table 16. Total temperature change due to flux divergence in the interval $50 < \nu < 2000$ cm^{-1}.

Level	No Cloud Cover $(\partial T/\partial t)$ °C day	Cloud Cover at Top $(\partial T/\partial t)$ °C day
	Sounding No. 1	
1–2	− .755	−.452
2–3	− .790	−.434
3–4	− .913	−.453
4–5	−1.141	−.471
5–6	−1.398	−.638
6–7	−1.197	−.513
7–8	− .888	−.251
8–9	− .978	−.231
9–10	−1.794	−.244
10–11	−1.756	−.150
11–12	−5.400	+.044
	Sounding No. 2	
1–2	− .737	−.564
2–3	− .731	−.513
3–4	− .845	−.568
4–5	− .874	−.486
5–6	−1.255	−.476
6–7	−2.548	−.803
7–8	−3.427	−.861
8–9	−2.460	−.235
9–10	−3.996	+.040

Table 16 (continued)

Level	No Cloud Cover ($\partial T/\partial t$) °C day	Cloud Cover at Top ($\partial T/\partial t$) °C day
	Sounding No. 3	
1–2	− .832	−.675
2–3	− .657	−.469
3–4	− .556	−.343
4–5	− .876	−.482
5–6	−1.925	−.880
6–7	−2.000	−.789
7–8	−2.043	−.524
8–9	−2.560	−.210
9–10	−3.041	+.029
	Sounding No. 4	
1–2	− .278	−.021
2–3	− .686	−.360
3–4	−1.446	−1.022
4–5	−1.115	−.651
5–6	−1.055	−.388
6–7	−1.490	−.196
7–8	−2.393	−.119
8–9	−4.309	+.047

BIBLIOGRAPHY

1. Cowling, T. G., 1950: Phil. Mag., 41, p. 109.

2. Curtis, A. R.,1952: Discussion of Goody's "A statistical model for water-vapour absorption." Quart. J. R. M. S., 78, p. 638.

3. Diermendjian, D., 1960: Atmospheric extinction of infra-red radiation. Quart. J. R. M. S., Vol. 86, July 1960.

4. Elsasser, W. M., 1942: Heat transfer by infrared radiation in the atmosphere. Harvard Meteor. Stud., No. 6.

5. Elsasser, W. M., 1960: Atmospheric radiation tables. Contract No. AF 19(604)-2413.

6. Godson, W. L., 1953: Spectral models and the properties of transmission functions. Proc. Toronto Meteor. Conference, pp. 35-42.

7. Goody, R. M., 1952: A statistical model for water-vapour absorption. Quart. J. R. M. S., 78, pp. 165-169.

8. Howard, J. N., Burch, D. L., Williams, D., 1955: Near-infrared transmission through synthetic atmospheres. Geophysical Research Directorate, Geophys. Research Papers No. 40, AFCRC-TR-55-213, November 1955.

9. Johnson, John C., 1954: Physical Meteorology, Technology Press of M.I.T.

10. Kaplan, L. D., 1950: Line intensities and absorption for the 15-micron carbon dioxide band. J. of Chem. Phys., Vol. 18, No. 2, pp 186-189, February 1950.

11. Kaplan, L. D., 1952: On the calculation of atmospheric transmission

functions for the infrared. J. of Met., 9, 1952.

12. Kaplan, L. D., 1952: On the pressure dependence of radiative heat transfer in the atmosphere. J. of Met., 9, pp. 1-12.

13. Kaplan, L. D., 1959: A method for calculation of infrared flux for use in numerical models of atmospheric motion. Rossby Memorial Volume.

14. Palmer, C. H., 1960: Experimental transmission functions for the pure rotation band of water vapor. J. Optical Society of America, Vol. 50, No. 12, December 1960.

15. Roach, W. T. and R. M. Goody, 1958: Absorption and emission in the atmospheric window, Quart. J. R. M. S., Vol. 84, December 1958.

16. Twomey, S., Table of the Planck Function for Terrestrial Temperatures. Supported by National Aeronautics and Space Administration.

17. Wexler, R., 1959 (Dec.): Satellite observations of infrared radiation. Contract No. AF 19(604)-5968.

18. Wexler, R., 1960 (June): Satellite observations of infrared radiation. Contract No. AF 19(604)-5968.